IEEE Access
Multidisciplinary | Rapid Review | Open Access Journal

Received February 4, 2021, accepted February 16, 2021, date of publication February 19, 2021, date of current version March 1, 2021.

Digital Object Identifier 10.1109/ACCESS.2021.3060381

A Novel Tracking Control Algorithm With Finite-Time Disturbance Observer for a Class of Second-Order Nonlinear Systems and Its Applications

ANH TUAN VO, THANH NGUYEN TRUONG, AND HEE-JUN KANG
Department of Electrical, Electronic and Computer Engineering, University of Ulsan, Ulsan 44610, South Korea

Corresponding author: Hee-Jun Kang (hjkang@ulsan.ac.kr)

This research was supported by Basic Science Research Program through the National Research Foundation of Korea (NRF) funded by the Ministry of Education (NRF-2019R1D1A3A03103528).

ABSTRACT This study aims to build a novel tracking control algorithm using a finite-time disturbance observer which obtains fast convergence within a predetermined amount of time and strong stability for a class of second-order nonlinear systems. Firstly, a nonlinear sliding mode manifold with fast finite-time convergence is introduced. Then, according to the designed manifold for the guarantee of finite-time convergence and robustness stabilization, a nonlinear control algorithm based on theory of finite-time control is developed. Specifically, the information of the lumped uncertainty was achieved by a new finite-time Disturbance Observer (DO). Thanks to the synthetic advantages of the above techniques, the designed controller marked with powerful features including a practical design, fast convergence rate, high precision, a convergence of the control errors in finite-time, along with impressive small chattering in the control actions. Furthermore, the control proposal also eliminates the necessity of the upper boundary of the uncertainties affecting the system and its finite settling time can be estimated in advance by designating the appropriate design parameters. The finite-time stability of the proposed DO, sliding surface, and control algorithm has been fully confirmed by Lyapunov principle. Trajectory tracking simulation for a 3-DOF manipulator and trajectory tracking experiment for a Maglev System (MLS) has been performed under different operating conditions using MATLAB/SIMULINK to testify the effectiveness and feasibility of the suggested strategy.

INDEX TERMS Dual layers adaptive law, nonsingular fast terminal sliding mode control, finite-time disturbance observer, robotic manipulators, maglev systems.

I. INTRODUCTION

The nature of all physical systems is nonlinear. For example, Maglev Systems (MLSs) have unstable characteristics and are described by high nonlinear differential equations, robot manipulators with the presence of friction at the joint actuator, uncertain dynamics, noise sensor, or external disturbances, and many other nonlinear systems in technology. Each nonlinear system is widely applied in different fields. They can be mentioned as follows. Robots play an important role in manufacturing to improve the productivity and quality of products. Robots perform rescue missions, explore the ocean as well as appear in daily life with humans. Robots are required to operate reliably, safely, with high performance. MLSs have been successfully used for many applications in industry, military, transportation, and so on. For example, rocket-guiding projects, frictionless bearings, magnetic bearings, high-speed trains, wafer distribution systems, contactless melting, vibration isolation systems, micro-robotics, gyroscopes, and so on. Or the applications of other nonlinear systems such as helicopters, underwater vehicles, drones, inverted pendulums, etc. Therefore, developing advanced solutions to increase safety, quality, and reliability for nonlinear systems is a challenge for researchers. Especially, there is always the presence of disturbances, uncertain components, and even faults that affect the system. Consequently, the control methodologies

The associate editor coordinating the review of this manuscript and approving it for publication was Bing Li.

have been suggested [1]–[6]. The control algorithm can be classified into two categories, including active and passive control system. For example, they can be mentioned such as active Fault-Tolerant Controller (FTC) [2]–[4] and passive FTC [1], [5], [6].

For the passive control system, the system is constructed without estimating disturbances and uncertainties. Therefore, performance depends on strong characteristics to deal with external disturbances or uncertainties. Numerous approaches have been designed to manipulate nonlinear systems. The passive controllers have fast response with external disturbances and uncertainties. Due to the dependence on the robustness of the control method, the ability to deal with highly uncertain terms may be limited when it is not strong enough. Therefore, the applicability to real systems may be limited.

Unlike the passive method, the output forces of the active controller are continuously tuned according to estimation response of uncertain terms. That information will come from an observer such as High Gain Observer (HGO) [7], [8], Sliding Mode Observer (SMO) [9], Neural Network Observer NNO [10], [11], Disturbance Observers (DO) [12], [13], nonlinear observers [14], or High Order Sliding Mode Observer (HOSMO) [15], [16]. Therefore, performance will depend on the accuracy of the information. The active controllers with exact provided data will have performed better than passive systems as compensation from online control reconfiguration. Consequently, they are more appropriate for robot applications. However, if the data is not provided correctly, the system will run into instability and destruction. Accordingly, the design of the active controllers combined with an observer that remains a significant challenge for scientists.

Sliding Mode Control (SMC) is high robustness to perturbations or uncertainties. Unfortunately, SMC has three major defects: 1) serious chattering; 2) slow transient performance; 3) the requirement of the upper-bound values of uncertain components. For the first defect, researchers have paid great attention to developing effective techniques as [17], [18], High-Order SMC (HOSMC) [19]–[24]. HOSMC seems to be an effective technique for designing an integrated control system with an observer [25]. To eliminate/reduce chattering using HOSMC is the first uses continuous control signals by calculating the integral of the discontinuous control signal. According to this calculation, a continuous compensation component is then added to the control loop to degrade the impact of total uncertainty. However, the sliding gain of HOSMC is selected the same as the sliding gain of SMC. Moreover, convergence stability in finite-time cannot be guaranteed with a traditional HOSMC.

Obviously, active control algorithms will provide higher tracking accuracy than that of passive controllers if the estimated information exactly offers to the control loop. As a result, approximate methods have been developed to approximate unknown components affecting the system, they can refer to as Neural Network (NN) and Fuzzy Logic System (FLS) [26], [27], respectively. Feed-Forward Neural Network (FFNN) methods have been established to nonlinear systems in [28], [29]. In [30], approximations with FLS have been applied to build control methods and observers for those objects or used a Radial Basis Function NN (RBFNN) to approximate/estimate the dynamics of the robot manipulators in [23]. Fundamentally, intelligent learning methods can have a good estimate only when the unidentified function being estimated regarding the control signal and/or the system states. However, these manners usually generate big estimation errors like exterior disturbance. An effective alternative is to add an observer for approximate of the unidentified functions. By studying this trend, the result is that many types of observers have been developed in the literature. The approach of these observer-control methods is conducted as follows, 1) an observer is built to approximately obtain the unknown models of exterior disturbance or uncertainty components; 2) Then, these models are added to the dynamic model of the controlled objects. As a result, the controlled system can be achieved the exact dynamic model. Another reason to use a combination of observer and sliding mode controller is based on the stable condition of SMC, the gain values of the reaching law in SMC should be assigned bigger than the upper-boundary values of total uncertainties [31]. Unfortunately, large gain values will make chattering happen seriously which should be overcome in a real system. For this problem, the effects of total uncertainties on the system must be reduced to the lowest possible level. Therefore, DO is often incorporated into SMC methods for offsetting the effects of total uncertainties and it also contributes to cut down the chattering phenomena [32]–[35]. However, the finite-time or fixed-time convergence of DO has not guaranteed or mentioned yet in those studies. Accordingly, the requirement is that the observer must have a finite-time convergence to avoid delay in supplying information to the control system. In addition, several observer-based control methods can provide convergence in a finite time. Unfortunately, their effectiveness has not been verified by experimental results such as [1] or [30]. This is also our motivation to propose a finite-time DO and its effectiveness will be fully verified by experiments under different conditions.

For the second defect, to enhance the transient and dynamic performance of SMC, the Fast Terminal SMC (FTSMC) or Global FTSMC (GFTSMC) have been proposed. These might guarantee the control errors of the system approaching zero value in a faster period of time along with finite-time convergence [36]. FTSMC has been of great interest to scientists and have been widely applied in practice. For example, global FTSMC schemes have been proposed for second-order systems or robot manipulators [37]–[41]. The control methods are developed based on Terminal SMC (TSMC) which provides the effective control performance in finite-time for nonlinear systems such as the finite-time control [42], Integral TSMC (ITSMC) [43], or Non-Singular Fast ITSMC (NFITSMC) [44].

For the last defect, many control algorithms based on SMC and FTSMC have been suggested using adaptive

laws to achieve efficiency in a simple way. By using the adaptive rules, the control parameters can be optimally adjusted to correspond to the effects of total uncertainties [45]–[47], [48]–[50]. Moreover, several intelligent calculating manners combined with SMC as NNs [51]–[53] and FLSs [54]–[56] have been recommended. Those can arbitrarily approximate any nonlinear components of the system. However, the use of these methods has a certain complexity as they increase the calculation in controlling design. Therefore, the adaptive methods are considered suitable for practical applications.

This study aims to build a novel tracking control algorithm using a finite-time disturbance observer which obtains fast convergence within a predetermined amount of time and strong stability for a class of second-order nonlinear systems. The proposed controller marked with powerful features and important contributions as follows:

1) A new adaptive DO with finite-time convergence has been developed to avoid delay in the information delivery of uncertain terms to the closed-loop system. This observer is developed based on HOSMO and dual layers adaptive rule. Therefore, it can significantly reduce chattering phenomena and remove the requirement of the upper bound of the lumped uncertainties.
2) The proposed control system has a practical design, fast convergence rate, high precision, a convergence of the control errors in finite-time, fast transient response along with impressive small chattering phenomena in control torque.
3) The proposed method is highly applicable in tracking control of a class of second-order nonlinear systems to follow the desired path despite the influences of uncertain dynamics or exterior disturbances.
4) The control parameters can be optimally adjusted to correspond to the effects of total uncertainties and the finite settling time of the control algorithm can be estimated in advance by designating the appropriate design parameters.
5) The Finite-time stability and robustness of the proposed DO, sliding surface, and control algorithm has been fully confirmed by Lyapunov principle, simulation for a 3-DOF manipulator, and trajectory tracking experiment for an MLS under different operating conditions.

The organization of our paper is as follows: Following the introduction in section 1 is the problem formulation. Section 3 describes the process of synthesizing controllers, analyzing stability, and proofs. Trajectory tracking simulation for a 3-DOF manipulator which is designed according to [57], [58] and trajectory tracking experimental for a MLS [59] have been performed under different operating conditions using MATLAB/SIMULINK along with discussions in comparing the performance of the proposed controller with other methods to investigate the powerful features of the design method in section 4. Finally, this work is closed with the conclusions.

II. FORMULATION OF THE PROBLEM AND PRELIMINARIES

A. MODELING OF THE NONLINEAR SYSTEMS

A class of second-order nonlinear systems is depicted in state space by:

$$\begin{cases} \dot{x}_1 = x_2 \\ \dot{x}_2 = a(x)\,u + b(x) + \Sigma(t), \end{cases} \tag{1}$$

where x_1, x_2 are state variables, $a(x)$ and $b(x)$ indicate dynamic nonlinear smooth functions that have the corresponding expression as $b(x) = b_n(x) + \delta b(x)$ with $b(0) = 0$, and $a(x)\,u = a(x)\,u_d + a(x)\,\delta u$. The term $\delta b(x)$ is an uncertain term. u is the real control signal, u_d is the designed control signal, and δu is an uncertainty of the input signal, while $\Sigma(t)$ indicates the lumped disturbance.

Entire uncertain terms are defined as the following function:

$$\Delta(x, \Sigma, t) = \delta b(x) + a(x)\,\delta u + \Sigma(t). \tag{2}$$

With Eq. (2), a full model of a class of second-order nonlinear systems is rearranged without loss of generality, as follows:

$$\begin{cases} \dot{x}_1 = x_2 \\ \dot{x}_2 = a(x)\,u_d + b_n(x) + \Delta(x, \Sigma, t). \end{cases} \tag{3}$$

Remark 1: For more convenience and duplication, entire uncertain terms will be handled as the lumped uncertainty. Because the lumped uncertainty has finite energy, therefore, it always has a bound value as the following assumptions [60]:

Assumption 1: The lumped uncertainty is bounded by:

$$|\Delta(x, \Sigma, t)| < \bar{\Delta}, \tag{4}$$

where $\bar{\Delta}$ is an upper bound value of the lumped uncertainty which is a positive constant.

Assumption 2: The first derivative of the lumped uncertainty is also bounded by:

$$\left|\dot{\Delta}(x, \Sigma, t)\right| < \Delta^*, \tag{5}$$

where Δ^* an unknown positive constant.

It is noted that the assumptions presented in Eqs. (4) and (5) are widely applied in the control design approach that appears in a lot of previous research in the literature [1], [61]. With the above assumptions, the Lipschitz condition is supposed to be practically satisfied in the bounded region of state space.

With the above problem statement, this study constructs a novel tracking control algorithm using a finite-time DO which obtains fast convergence within a predetermined amount of time and strong stability for a class of second-order nonlinear systems. The proposed controller should achieve the following control objectives, such as nonsingular, chattering reduction, fast stabilization in finite-time, and improved control performance compared to the existing finite-time control algorithms.

B. PRELIMINARY CONCEPTS

Consider the following system:

$$\dot{x}(t) = f(t, x), \quad x(0) = x_0, \tag{6}$$

where $x \in R^n, f(x)$: Δ is nonlinear function that is on open neighborhood $\Delta \subseteq R^n$ of the origin, and $f(0) = 0$. The origin is assumed to be an equilibrium point of the system (6).

Definition 1: The origin point of the system (6) is called to be a globally finite-time stable if it is globally asymptotically stable with bounded time function $T(x_0)$, i.e., there exists $T_{\max} > 0$ such that $T(x_0)$ satisfies the term $T(x_0) < T_{\max}$.

Lemma 1 [41]: Consider a differential equation:

$$\dot{q} = -\frac{2\alpha_0}{1 + e^{-\eta_0(|q|-\varepsilon_0)}} q - \frac{2\beta_0}{1 + e^{\mu_0(|q|-\varepsilon_0)}} sig(q)^{\omega_0}, \tag{7}$$

where $\alpha_0, \beta_0, \eta_0, \mu_0$ are the designated positive constants, $0 < \omega_0 < 1$, $\varepsilon_0 = \left(\beta_0/\alpha_0\right)^{1/(1-\omega_0)}$, and $sig(q)^{\omega_0} = |q|^{\omega_0} \operatorname{sgn}(q)$. Accordingly, the dynamic (7) is declared as finite-time stabilization with respect to the initial term $q(0)$ and the settling time T_0 is given by:

$$T_0 < \frac{\ln(|q(0)|) - \ln(\varepsilon_0)}{\alpha_0} + \frac{1}{\beta_0(1-\delta_0)} |\varepsilon_0|^{1-\omega_0}. \tag{8}$$

Lemma 2 [62]: Consider a differential equation:

$$\dot{q} = -\alpha_0 sig(q)^{\eta_0} - \beta_0 sig(q)^{\mu_0}, \tag{9}$$

where α_0, β_0 are the selected positive constants, $sig(q)^{\gamma_i} = |q|^{\gamma_i} \operatorname{sgn}(q)$, $\eta_0 = \frac{(\varphi_0+1)}{2} + \frac{(\varphi_0-1)\operatorname{sgn}(|q|-1)}{2}$, $\mu_0 = \frac{(\varphi_0+\lambda_0)}{2} + \frac{(\varphi_0-\lambda_0)\operatorname{sgn}(|q|-1)}{2}$, $\varphi_0 > 1$, and $0 < \lambda_0 < 1$. Therefore, dynamic (9) is acknowledged as finite-time stabilization with respect to the initial term $q(0)$ and the settling time T_0 is given by:

$$T_0 < \frac{1}{(\alpha_0+\beta_0)(\varphi_0-1)} + \frac{1}{\beta_0(1-\lambda_0)} \ln\left(1 + \frac{\alpha_0}{\beta_0}\right). \tag{10}$$

III. CONTROL DESIGN AND STABILITY INVESTIGATION

This section presents tracking control of a class of second-order nonlinear systems which ensures fast finite-time stability and high tracking performance. The control design procedure is carried out in the following main steps. First, a new DO is proposed based on a combination of DO, HOSMO, and dual layers adaptive rule. The proposed observer can provide a finite-time convergence to avoid delay in the information delivery of uncertain terms to the closed-loop system. Second, the finite-time sliding surface is designed to achieve fast finite-time convergence and improve dynamic performance. Finally, a new finite-time control based on the proposed DO and finite-time sliding surface, which can guarantee convergence of the control errors in finite-time, is proposed.

A. DESIGN OF THE PROPOSED DISTURBANCE OBSERVER

$$\begin{cases} \tilde{\upsilon} = \upsilon - x_2 \\ \dot{\upsilon} = a(x) u_d + b_n(x) + \hat{\Delta} \\ \quad - \dfrac{2\alpha_3}{1 + e^{-\eta_3(|\tilde{\upsilon}|-\varepsilon_3)}} \tilde{\upsilon} - \dfrac{2\beta_3}{1 + e^{\mu_3(|\tilde{\upsilon}|-\varepsilon_3)}} sig(\tilde{\upsilon})^{\omega_3}, \end{cases} \tag{11}$$

where υ indicates an approximated value of x_2. Additionally, $\alpha_3, \beta_3, \eta_3, \mu_3$ are the designated positive constants, $0 < \omega_3 < 1$, and $\varepsilon_3 = \left(\beta_3/\alpha_3\right)^{1/(1-\omega_3)}$. The term of $\hat{\Delta}$ approximated value of the lumped uncertainty and the corresponding updating rule is designed as follows:

$$\begin{cases} \varpi = \dot{\tilde{\upsilon}} + \dfrac{2\alpha_3}{1 + e^{-\eta_3(|\tilde{\upsilon}|-\varepsilon_3)}} \tilde{\upsilon} + \dfrac{2\beta_3}{1 + e^{\mu_3(|\tilde{\upsilon}|-\varepsilon_3)}} sig(\tilde{\upsilon})^{\omega_3} \\ \dot{\hat{\Delta}} = -\dfrac{2\alpha_4}{1 + e^{-\eta_4(|\varpi|-\varepsilon_4)}} \varpi - \dfrac{2\beta_4}{1 + e^{\mu_4(|\varpi|-\varepsilon_4)}} sig(\varpi)^{\omega_4} \\ \quad - \Delta^*(t) \operatorname{sgn}(\varpi), \end{cases} \tag{12}$$

where $\alpha_4, \beta_4, \eta_4, \mu_4$ are the designated positive constants, $0 < \omega_4 < 1$, $\varepsilon_4 = \left(\beta_4/\alpha_4\right)^{1/(1-\omega_4)}$, and $\Delta^*(t)$ is an adaptation gain value.

Theorem 1: We consider the dynamical system (3) if a DO is proposed as Eq. (11) and its corresponding updating rule as Eq. (12) to approximate the lumped uncertainty along with the term $\Delta^*(t) > \left|\dot{\Delta}(x, \Sigma, t)\right|$ then DO's approximation error will reach zero in finite-time.

The Validity of Theorem 1:

Taking the first derivative of the term $\tilde{\upsilon}$ based on Eqs. (11) - (12) obtains:

$$\begin{aligned} \dot{\tilde{\upsilon}} &= \dot{\upsilon} - \dot{x}_2 \\ &= \hat{\Delta} - \Delta - \frac{2\alpha_3}{1 + e^{-\eta_3(|\tilde{\upsilon}|-\varepsilon_3)}} \tilde{\upsilon} - \frac{2\beta_3}{1 + e^{\mu_3(|\tilde{\upsilon}|-\varepsilon_3)}} sig(\tilde{\upsilon})^{\omega_3}. \end{aligned} \tag{13}$$

Substituting Eq. (13) into Eq. (12) then taking time derivative of the obtained result, we achieve:

$$\begin{cases} \varpi = \hat{\Delta} - \Delta \\ \dot{\varpi} = -\dot{\Delta} - \Delta^*(t) \operatorname{sgn}(\varpi) \\ -\dfrac{2\alpha_4}{1 + e^{-\eta_4(|\varpi|-\varepsilon_4)}} \varpi - \dfrac{2\beta_4}{1 + e^{\mu_4(|\varpi|-\varepsilon_4)}} sig(\varpi)^{\omega_4}. \end{cases} \tag{14}$$

Defining a Lyapunov function $V_1 = 0.5\varpi^2$ and calculating its time derivative along with the result in Eq. (14) as follows:

$$\begin{aligned} \dot{V}_1 &= \varpi\dot{\varpi} \\ &= \varpi \begin{pmatrix} -\dot{\Delta} - \dfrac{2\alpha_4}{1 + e^{-\eta_4(|\varpi|-\varepsilon_4)}} \varpi \\ -\dfrac{2\beta_4}{1 + e^{\mu_4(|\varpi|-\varepsilon_4)}} |\varpi|^{\omega_4} \operatorname{sgn}(\varpi) \\ -\Delta^*(t) \operatorname{sgn}(\varpi) \end{pmatrix} \\ &= -\dot{\Delta}\varpi - \Delta^*(t)|\varpi| - \frac{2\alpha_4}{1 + e^{-\eta_4(|\varpi|-\varepsilon_4)}} \varpi^2 \\ &\quad - \frac{2\beta_4}{1 + e^{\mu_4(|\varpi|-\varepsilon_4)}} |\varpi|^{\omega_4+1} \\ &\leqslant -\left(\Delta^*(t) - \left|\dot{\Delta}\right|\right)|\varpi| - \frac{2\alpha_4}{1 + e^{-\eta_4(|\varpi|-\varepsilon_4)}} \varpi^2 \\ &\quad - \frac{2\beta_4}{1 + e^{\mu_4(|\varpi|-\varepsilon_4)}} |\varpi|^{\omega_4+1} \\ &\leqslant -\frac{2\alpha_4}{1 + e^{-\eta_4(|\varpi|-\varepsilon_4)}} \varpi^2 - \frac{2\beta_4}{1 + e^{\mu_4(|\varpi|-\varepsilon_4)}} |\varpi|^{\omega_4+1} \\ &\leqslant 0. \end{aligned} \tag{15}$$

Since the condition $V_1 > 0$ and $\dot{V}_1 \leqslant 0$ is guaranteed. Accordingly, the sliding mode surface ϖ selected for DO will reach zero in finite-time, i.e., $\varpi = 0$.

We define $\tilde{\Delta} = \hat{\Delta} - \Delta$ as DO's approximation error from Eq. (14) as follows:

$$\tilde{\Delta} = \hat{\Delta} - \Delta = \varpi. \tag{16}$$

Once $\varpi = 0$ then $\tilde{\Delta} = \varpi = 0$. Obviously, the proposed DO can approximate the lumped uncertainty in finite-time.

This completes the evidence.

To guarantee the stability condition for the system (3), the design parameter of $\Delta^*(t)$ is chosen according to Assumption 2. However, the choice of this parameter is not easy in practice because of the existence of uncertain components affecting the system. To overcome that problem and to eliminate the requirement of the foreseeable knowledge of all uncertain terms, we can apply the approximation or adaptive techniques to obtain the approximation values. Therefore, the value $\Delta^*(t)$ in this paper is obtained with the dual layers adaptive law as in [63,64]:

$$\begin{cases} \dot{\Delta}^*(t) = -(\Delta_0 + \Delta_1)\,\mathrm{sgn}(\psi) \\ \dot{\Delta}_1(t) = \begin{cases} \Delta_d\,|\psi|, & |\psi| > \psi_0 \\ 0, & |\psi| \leqslant \psi_0 \end{cases} \end{cases} \tag{17}$$

in which

$$\begin{cases} \psi = \Delta^*(t) - \dfrac{|\xi|}{k_0} - k_1 \\ \dot{\xi} = \rho fal\left(-\Delta^*(t)\,\mathrm{sgn}(\varpi) - \xi, \kappa, \theta\right) \\ fal(\Psi, \kappa, \theta) = \begin{cases} |\Psi|^{\kappa}\,\mathrm{sgn}(\Psi), & |\Psi| > \theta \\ \dfrac{\Psi}{\theta^{1-\kappa}}, & |\Psi| \leqslant \theta, \end{cases} \end{cases} \tag{18}$$

where $\Delta_0, \Delta_d, \rho > 0$ and $0 < k_0, k_1, \kappa, \theta$. An approximation value of $-\Delta^*(t)\,\mathrm{sgn}(\varpi)$ can be achieved by the $fal(\cdot)$ function filter in real-time.

B. DESIGN OF THE PROPOSED FINITE-TIME SLIDING MODE SURFACE

Let $x_r = \left[x_{1r}, \ldots, x_{nr}\right]^T \in R^n$ be the vector of the prescribed reference path. Therefore, $x_e = x_1 - x_r$ is the positional control error and $\dot{x}_e = \dot{x}_1 - \dot{x}_r$ is the velocity control error.

From the positional control error, we design a finite-time sliding mode surface based on Lemma 1 as:

$$s = \dot{x}_e + \frac{2\alpha_1}{1 + e^{-\eta_1(|x_e| - \varepsilon_1)}} x_e + \frac{2\beta_1}{1 + e^{\mu_1(|x_e| - \varepsilon_1)}} sig(x_e)^{\omega_1}, \tag{19}$$

where $s \in R^{n\times 1}$ is the sliding mode surface, $\alpha_1, \beta_1, \eta_1, \mu_1$ are the design positive constants, $0 < \omega_1 < 1$, $\varepsilon_1 = \left(\beta_1/\alpha_1\right)^{1/(1-\omega_1)}$, and $sig(x_e)^{\omega_1} = |x_e|^{\omega_1}\,\mathrm{sgn}(x_e)$.

Once the system states run in the sliding motion phase, they must be satisfied condition [65], i.e., $s = 0$. Therefore, we consider equation (19) in case of $s = 0$ as follows:

$$\dot{x}_e = -\frac{2\alpha_1}{1 + e^{-\eta_1(|x_e| - \varepsilon_1)}} x_e - \frac{2\beta_1}{1 + e^{\mu_1(|x_e| - \varepsilon_1)}} sig(x_e)^{\omega_1}. \tag{20}$$

Theorem 1: Let us investigate the dynamics (20) with the equilibrium point, $x_e = 0$, and the state variables of the dynamic (20), $x_e = 0$, within the finite time $T_s < \frac{\ln(|x_e(0)|) - \ln(\varepsilon_1)}{\alpha_1} + \frac{1}{\beta_1(1-\delta_1)}|\varepsilon_1|^{1-\omega_1}$.

Remark 2: The role of each nonlinear term in dynamic (20) is determined as follows: the first nonlinear term plays a major role in stage $x_e(0) \to |x_e| = \varepsilon_1$; the second nonlinear term plays a major role in stage $|x_e| = \varepsilon_1 \to x_e = 0$.

Proof of the Correctness of Statement in Theorem 1:

By combining both phases and based on Remark 1, the finite settling time of the sliding motion is calculated by:

$$\begin{aligned} T_s &< \int_{\varepsilon_1}^{x_e(0)} \frac{1}{\alpha_1 |x_e|} d(|x_e|) + \int_0^{\varepsilon_1} \frac{1}{\beta_1 |x_e|^{\delta_1}} d(|x_e|) \\ &< \frac{\ln(|x_e(0)|) - \ln(\varepsilon_1)}{\alpha_1} + \frac{1}{\beta_1(1 - \delta_1)} |\varepsilon_1|^{1-\omega_1}. \end{aligned} \tag{21}$$

This completes the evidence.

C. CONTROL DESIGN SYNTHESIS OF THE CONTROL PROPOSAL

This subsection presents a novel tracking control algorithm which is devised based on the designed DO in Eq. (11) and the proposed sliding mode surface in Eq. (19) to achieve high control performance for the system (3).

To achieve the effective control input, Eq. (19) is firstly differentiated with respect to time as:

$$\begin{aligned} \dot{s} = \ddot{x}_e &+ \frac{2\alpha_1}{1 + e^{-\eta_1(|x_e| - \varepsilon_1)}} \dot{x}_e \\ &+ \frac{2\alpha_1 \eta_1 \dot{x}_e\,\mathrm{sgn}(x_e)\, e^{-\eta_1(|x_e| - \varepsilon_1)}}{\left(1 + e^{-\eta_1(|x_e| - \varepsilon_1)}\right)^2} x_e \\ &+ \frac{2\beta_1\omega_1}{1 + e^{\mu_1(|x_e| - \varepsilon_1)}} |x_e|^{\omega_1 - 1} \dot{x}_e \\ &- \frac{2\beta_1\mu_1\dot{x}_e e^{\mu_1(|x_e| - \varepsilon_1)}}{\left(1 + e^{\mu_1(|x_e| - \varepsilon_1)}\right)^2} |x_e|^{\omega_1}. \end{aligned} \tag{22}$$

With $\ddot{x}_e = \dot{x}_2 - \ddot{x}_r$, the dynamic (22) can then rewrite along with the system (3) as:

$$\begin{aligned} \dot{s} = a(x)\,u_d + b_n(x) + \Delta(x, \Sigma, t) - \ddot{x}_r \\ + \frac{2\alpha_1}{1 + e^{-\eta_1(|x_e| - \varepsilon_1)}} \dot{x}_e + \frac{2\alpha_1 \eta_1 \dot{x}_e\,\mathrm{sgn}(x_e)\, e^{-\eta_1(|x_e| - \varepsilon_1)}}{\left(1 + e^{-\eta_1(|x_e| - \varepsilon_1)}\right)^2} x_e \\ + \frac{2\beta_1\omega_1}{1 + e^{\mu_1(|x_e| - \varepsilon_1)}} |x_e|^{\omega_1 - 1} \dot{x}_e - \frac{2\beta_1\mu_1\dot{x}_e e^{\mu_1(|x_e| - \varepsilon_1)}}{\left(1 + e^{\mu_1(|x_e| - \varepsilon_1)}\right)^2} |x_e|^{\omega_1}. \end{aligned} \tag{23}$$

Finally, the control signals are formed as:

$$u_d = -\frac{1}{a(x)}\left(u_{eq} + u_r\right), \tag{24}$$

where the term of u_{eq}, guarantees the pathway of the control errors on the sliding surface (19) and handles the

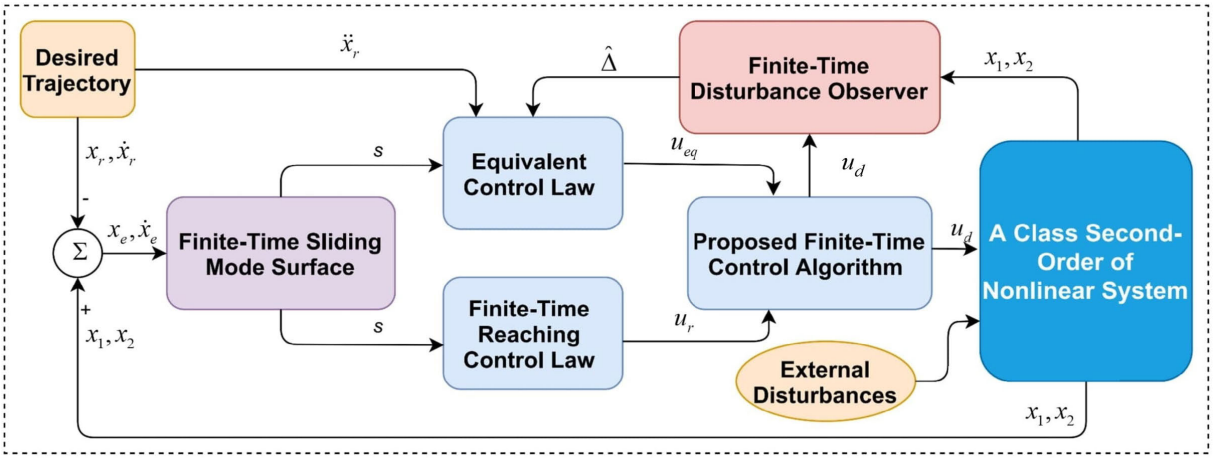

FIGURE 1. Diagram of the proposed control algorithm.

lumped uncertainty. u_{eq} is constructed from DO (11) and dynamic (23) as:

$$\begin{aligned} u_{eq} = {} & b_n(x) + \hat{\Delta} - \ddot{x}_r + \frac{2\alpha_1}{1+e^{-\eta_1(|x_e|-\varepsilon_1)}}\dot{x}_e \\ & + \frac{2\alpha_1\eta_1\dot{x}_e \operatorname{sgn}(x_e)\, e^{-\eta_1(|x_e|-\varepsilon_1)}}{\left(1+e^{-\eta_1(|x_e|-\varepsilon_1)}\right)^2}x_e \\ & + \frac{2\beta_1\omega_1}{1+e^{\mu_1(|x_e|-\varepsilon_1)}}|x_e|^{\omega_1-1}\dot{x}_e \\ & - \frac{2\beta_1\mu_1\dot{x}_e e^{\mu_1(|x_e|-\varepsilon_1)}}{\left(1+e^{\mu_1(|x_e|-\varepsilon_1)}\right)^2}|x_e|^{\omega_1}. \end{aligned} \tag{25}$$

To handle the remaining influences from the term $\tilde{\Delta}$ and to provide a fast convergence for the system trajectory in approaching the proposed sliding mode surface, the reaching control law is suggested in the below expression:

$$u_r = \alpha_2 sig(s)^{\eta_2} + \beta_2 sig(s)^{\mu_2}, \tag{26}$$

where α_2, β_2 are the design positive constants, $sig(s)^{\gamma_i} = |s|^{\gamma_i}\operatorname{sgn}(s)$, $\eta_2 = \frac{(\varphi_2+1)}{2} + \frac{(\varphi_2-1)\operatorname{sgn}(|s|-1)}{2}$, $\mu_2 = \frac{(\varphi_2+\lambda_2)}{2} + \frac{(\varphi_2-\lambda_2)\operatorname{sgn}(|s|-1)}{2}$, $\varphi_2 > 1$, and $0 < \lambda_2 < 1$.

Proof of Stability of the Control Proposal:

Utilizing the control input signals (24) - (26) to the expression in Eq. (23) offers:

$$\dot{s} = -u_r - \tilde{\Delta}. \tag{27}$$

The following Lyapunov candidate $V_2 = s^2$ is considered to verify correctness of the suggested control input (24) and its time derivative is calculated as:

$$\begin{aligned} \dot{V}_2 &= 2s\dot{s} \\ &= 2s\left(-u_r - \tilde{\Delta}\right) \\ &= 2s\left(-\alpha_2|s|^{\eta_2}\operatorname{sgn}(s) - \beta_2|s|^{\mu_2}\operatorname{sgn}(s) - \tilde{\Delta}\right) \\ &= -2\alpha_2|s|^{\eta_2+1} - 2\beta_2|s|^{\mu_2+1} - 2\tilde{\Delta}s. \end{aligned} \tag{28}$$

As concluded in the stability analysis of the proposed DO, DO can estimate the lumped uncertainty in finite-time. It is means that there exists a finite-time $\bar{T}$ such that $\tilde{\Delta} = 0$ for $t > \bar{T}$, then,

$$\begin{aligned} \dot{V}_2 &= -2\alpha_2|s|^{\eta_2+1} - 2\beta_2|s|^{\mu_2+1} \\ &= -2\alpha_2 V_2^{\frac{\eta_2+1}{2}} - 2\beta_2 V_2^{\frac{\mu_2+1}{2}}. \end{aligned} \tag{29}$$

Based on Lemma 2, the proposed sliding mode surface will be converged to zero in finite-time T_r and the convergence time T_r is bounded by:

$$T_r < \frac{1}{(\alpha_2+\beta_2)(\varphi_2-1)} + \frac{1}{\beta_2(1-\lambda_2)}\ln\left(1+\frac{\alpha_2}{\beta_2}\right). \tag{30}$$

Therefore, the total convergence time for the system (3) can be defined as

$$\begin{aligned} T &= T_r + T_s \\ &< \frac{1}{(\alpha_2+\beta_2)(\varphi_2-1)} + \frac{1}{\beta_2(1-\lambda_2)}\ln\left(1+\frac{\alpha_2}{\beta_2}\right) \\ &\quad + \frac{\ln(|x_e(0)|) - \ln(\varepsilon_1)}{\alpha_1} + \frac{1}{\beta_1(1-\delta_1)}|\varepsilon_1|^{1-\omega_1}. \end{aligned} \tag{31}$$

This completes the evidence.

Block Diagram of the designed control system is illustrated in Fig. 1.

IV. SIMULATION RESULTS AND DISCUSSION

Trajectory tracking simulation for a 3-DOF robotic manipulator which is designed according to [57] and trajectory tracking experimental for an MLS [59] have been performed using MATLAB/SIMULINK along with discussions in comparing the performance of the proposed controller with other similar methods as non-singular FTSMC (NFTSMC) [66] and NFTSMC [41] to validate the superior performance of the proposed algorithm.

A. COMPUTER SIMULATION FOR TRAJECTORY TRACKING CONTROL OF AN UNCERTAIN 3-DOF ROBOTIC MANIPULATOR

A 3-DOF robotic manipulator has been performed for all simulation investigations by using MATLAB/SIMULINK and SOLIDWORKS. The kinematic description and dynamic calculation of the robot are based on [57, 58]. All the mechanical components of this robot were firstly designed by using SOLIDWORKS software. Those were then introduced into the SOLIDWORKS assembly environment to add the coordinate system, complete construction of the robot, and find the direction of gravitational force. Next, using the Simscape Multibody Link Tool of the SOLIDWORKS to export an XML file and STEP files. The XML file contains essential parameters of the robot's mechanical components, including mass, inertia moment, the center of mass, as well as all parameters of the coordinate system of the assembly environment. STEP files contain the 3-D computer-aided design (CAD) model of the mechanical components. Finally, whole files are embedded into the MATLAB/SIMULINK environment using Simscape Multibody Link. As a result, the achieved robot model will be completely like the actual dynamic model. The lumped uncertainty including unknown dynamic model, disturbance, and friction are also assumed to impact the system for testing control performance, as follows.

Consider the modelling of the robot dynamic explained in joint space by:

$$M(p)\ddot{p} + C(p,\dot{p})\dot{p} + G(p) + F_r(\dot{p}) = \tau - \tau_d(t), \quad (32)$$

where $p \in R^{3\times1}, \dot{p} \in R^{3\times1}$, and $\ddot{p} \in R^{3\times1}$ are corresponding to the vector of position, velocity, and acceleration in joint space. $M(p) \in R^{3\times3}$, $C(p,\dot{p}) \in R^{3\times3}$, and $G(p) \in R^{3\times1}$ are corresponding to the matrix of mass, Coriolis and centrifugal forces, and gravitational force. $\tau \in R^{3\times1}$, $F_r(\dot{p}) \in R^{3\times1}$, and $\tau_d(t) \in R^{3\times1}$ are corresponding to the vector of the control torque, friction force, and the lumped disturbance.

In fact, it is not easy to achieve a precise dynamic model of the robot. Therefore, we assume that:

$$\begin{cases} M(p) = \hat{M}(p) + dM(p) \\ C(p,\dot{p}) = \hat{C}(p,\dot{p}) + dC(p,\dot{p}) \\ G(p) = \hat{G}(p) + dG(p), \end{cases} \quad (33)$$

where $\hat{M}(p) \in R^{3\times3}$, $\hat{C}(p,\dot{p}) \in R^{3\times3}$, and $\hat{G}(p) \in R^{3\times1}$ are corresponding to estimation values of the real values of $M(p)$, $C(p,\dot{p})$, and $G(p)$. $dM(p) \in R^{3\times3}$, $dC(p,\dot{p}) \in R^{3\times3}$, and $dG(p) \in R^{3\times1}$ are uncertain dynamics.

We set $x = \left[x_1^T, x_2^T\right]^T = \left[p^T, \dot{p}^T\right]^T$ and $u = \tau$; accordingly, the modelling of the robot dynamic (32) is depicted in state space by:

$$\begin{cases} \dot{x}_1 = x_2 \\ \dot{x}_2 = a(x)u + b(x) + \Delta(x,d,t), \end{cases} \quad (34)$$

where $b(x) = -\hat{M}^{-1}(p)\left(\hat{C}(p,\dot{p})\dot{p} + \hat{G}(p)\right)$ indicates the nominal of the robot, $a(x) = \hat{M}^{-1}(p)$ stands for a smooth function, while

$$\Delta(x,d,t) = -\hat{M}^{-1}(p)\begin{pmatrix} F_r(\dot{p}) + dM(p)\ddot{p} \\ +dC(p,\dot{p})\dot{p} + dG(p) + \tau_d(t) \end{pmatrix}$$

indicates the lumped uncertainty.

Eq. (34) has a form of a second-order nonlinear system. Therefore, the proposed method can be directly applied to this robot.

We assume that the unknown dynamic models are assigned as $dM(p) = 0.2M(p)$, $dC(p,\dot{p}) = 0.2C(p,\dot{p})$, and $dG(p) = 0.2G(p)$ for all cases of the simulation.

The friction and external disturbance were also modeled in the corresponding equations, as follows:

$$F_r(\dot{p}) = \begin{bmatrix} 0.1\text{sgn}(\dot{p}_1) + 2\dot{p}_1 \\ 0.1\text{sgn}(\dot{p}_2) + 2\dot{p}_2 \\ 0.1\text{sgn}(\dot{p}_3) + 2\dot{p}_3 \end{bmatrix} (N.m) \quad (35)$$

and

$$\tau_d(t) = \begin{bmatrix} 4\sin(t) \\ 5\sin(t) \\ 6\sin(t) \end{bmatrix} (N.m). \quad (36)$$

3D description of a 3-DOF robotic manipulator using SOLIDWORKS is illustrated in Fig. 2.

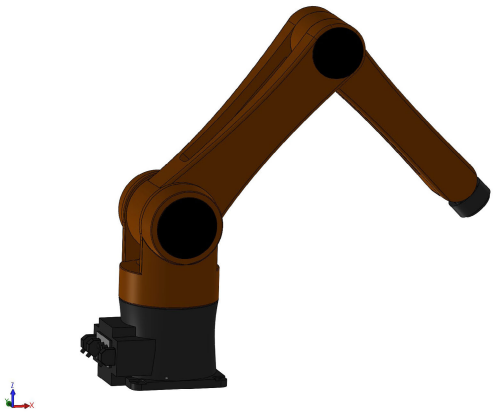

FIGURE 2. 3D description of a 3-DOF robotic manipulator using SOLIDWORKS.

The parameters of the robot system are set as follows. The corresponding mass of each link is $m_1 = 33.429\ (kg)$, $m_2 = 34.129\ (kg)$, and $m_3 = 15.612\ (kg)$; the corresponding length of each link is $l_1 = 0.25\ (m)$, $l_2 = 0.7\ (m)$, and $l_3 = 0.6\ (m)$; the corresponding center of mass of each link is $\left[l_{c1x}, l_{c1y}, l_{c1z}\right]^T = \left[0, 0, -74.610 \times 10^{-3}\right]^T\ (m)$, $\left[l_{c2x}, l_{c2y}, l_{c2z}\right]^T = [0.3477, 0, 0]^T\ (m)$, and $\left[l_{c3x}, l_{c3y}, l_{c3z}\right]^T = [0.3142, 0, 0]^T\ (m)$; the corresponding inertia of each link is $\left[I_{1xx}, I_{1yy}, I_{1zz}\right]^T = [0.7486, 0.5518, 0.5570]^T\ \left(kg.m^2\right)$, $\left[I_{2xx}, I_{2yy}, I_{2zz}\right]^T = [0.3080, 2.4655, 2.3938]^T\ \left(kg.m^2\right)$, and $\left[I_{3xx}, I_{3yy}, I_{3zz}\right]^T = [0.0446, 0.7092, 0.7207]^T\ \left(kg.m^2\right)$.

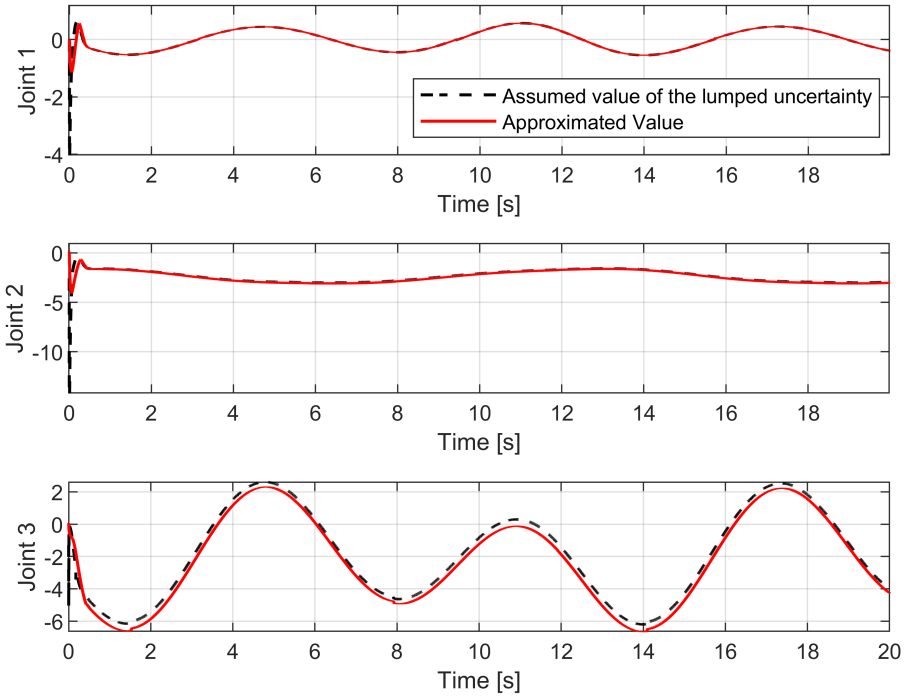

FIGURE 3. Assumed value of the lumped uncertainty and its approximation value at each Joint.

The robot's end-effector position is driven to follow the reference trajectory, as follows:

$$\begin{cases} x = 0.85 - 0.01t \\ y = 0.2 + 0.2\sin(0.5t) \\ z = 0.7 + 0.2\cos(0.5t) \end{cases} (m). \tag{37}$$

The control inputs of NFTSMC based [66] and NFTSMC based on [41] are synthesized for a 3-DOF robotic manipulator as:

$$\begin{cases} s = \dot{x}_e + \alpha_5 x_e + \beta_5 sig(x_e)^{\omega_5} \\ u_d = -\dfrac{1}{a(x)}\begin{pmatrix} b_n(x) + \left(\alpha_5 + \beta_5\omega_5|x_e|^{\omega_5 - 1}\right)\dot{x}_e \\ +\Lambda_5 s + \left(\Delta_5^* + v_5\right)\mathrm{sgn}(s) - \ddot{x}_r \end{pmatrix} \end{cases} \tag{38}$$

and

$$\begin{cases} s = \dot{x}_e + \dfrac{2\alpha_6}{1 + e^{-\eta_6(|x_e| - \varepsilon_6)}}x_e + \dfrac{2\beta_6}{1 + e^{\mu_6(|x_e| - \varepsilon_6)}}sig(x_e)^{\omega_6} \\ u_d = -\dfrac{1}{a(x)}\begin{pmatrix} b_n(x) + \dfrac{2\alpha_6}{1 + e^{-\eta_6(|x_e| - \varepsilon_6)}}\dot{x}_e \\ +\dfrac{2\alpha_6\eta_6\dot{x}_e\,\mathrm{sgn}(x_e)\,e^{-\eta_6(|x_e| - \varepsilon_6)}}{\left(1 + e^{-\eta_6(|x_e| - \varepsilon_6)}\right)^2}x_e \\ +\dfrac{2\beta_6\omega_6}{1 + e^{\mu_6(|x_e| - \varepsilon_6)}}|x_e|^{\omega_6 - 1}\dot{x}_e \\ -\dfrac{2\beta_6\mu_6\dot{x}_e e^{\mu_6(|x_e| - \varepsilon_6)}}{\left(1 + e^{\mu_6(|x_e| - \varepsilon_6)}\right)^2}|x_e|^{\omega_6} \\ +\Lambda_6 s + \left(\Delta_6^* + v_6\right)\mathrm{sgn}(s) - \ddot{x}_r \end{pmatrix} \end{cases}. \tag{39}$$

TABLE 1. Control parameter selection of control algorithms.

Algorithm	Control Parameters
NFTSMC1	$\alpha_5 = 5,\ \beta_5 = 5,\ \omega_5 = 0.8,\ \Lambda_5 = 5,\ \Delta_5^* = 13, v_5 = 0.1$
NFTSMC2	$\alpha_6 = 5,\ \beta_6 = 5,\ \eta_6 = 0.9, \mu_6 = 1.2, \omega_6 = 0.8, \Lambda_6 = 5,\ \Delta_6^* = 13, v_6 = 0.1$
Proposed Algorithm	Eq. (19): $\alpha_1 = 5,\ \beta_1 = 5,\ \eta_1 = 0.9,\ \mu_1 = 1.2, \omega_1 = 0.8$ Eq. (26): $\alpha_2 = 5,\ \beta_2 = 5,\ \varphi_2 = 1.7,\ \lambda_2 = 0.6$ Eqs. (11) and (12): $\alpha_3 = 6,\ \beta_3 = 6,\ \eta_3 = 0.9,\ \mu_3 = 1.2, \omega_3 = 0.7, \alpha_4 = 6,\ \beta_4 = 6,\ \eta_4 = 0.9,\ \mu_4 = 1.2, \omega_4 = 0.7$ Eqs. (17) and (18): $\Delta_0 = 5, \Delta_d = 20, \psi_0 = 0.7, \rho = 4, k_0 = 0.4, k_1 = 3, \kappa = 0.9, \theta = 0.7$

where $x_e = x - x_r$, $\alpha_5, \alpha_6, \beta_5, \beta_6, \eta_6, \mu_6$ are the design positive constants, $0 < \omega_5, \omega_6 < 1$, $\varepsilon_6 = \left(\beta_6/\alpha_6\right)^{1/(1-\omega_6)}$. $\left(\Delta_5^* + v_5\right)$ and $\left(\Delta_6^* + v_6\right)$ are positive constants.

Control parameter selection of the three control algorithms in a computer simulation is reported in Table 1.

First, we investigate the effectiveness of the proposed observer in approximating the lumped uncertainty. As shown in Fig. 3, the proposed DO has exactly approximated the assumed value of the lumped uncertainty in both amplitude and frequency. And it is especially important that the DO has convergence in finite-time. Consequently, it provides timely and accurate information about the uncertain components to the control system and this contributes to enhanced performance and reduces the dynamic computation burden.

Second, we consider the effectiveness of the proposed controller in trajectory tracking from the control performance

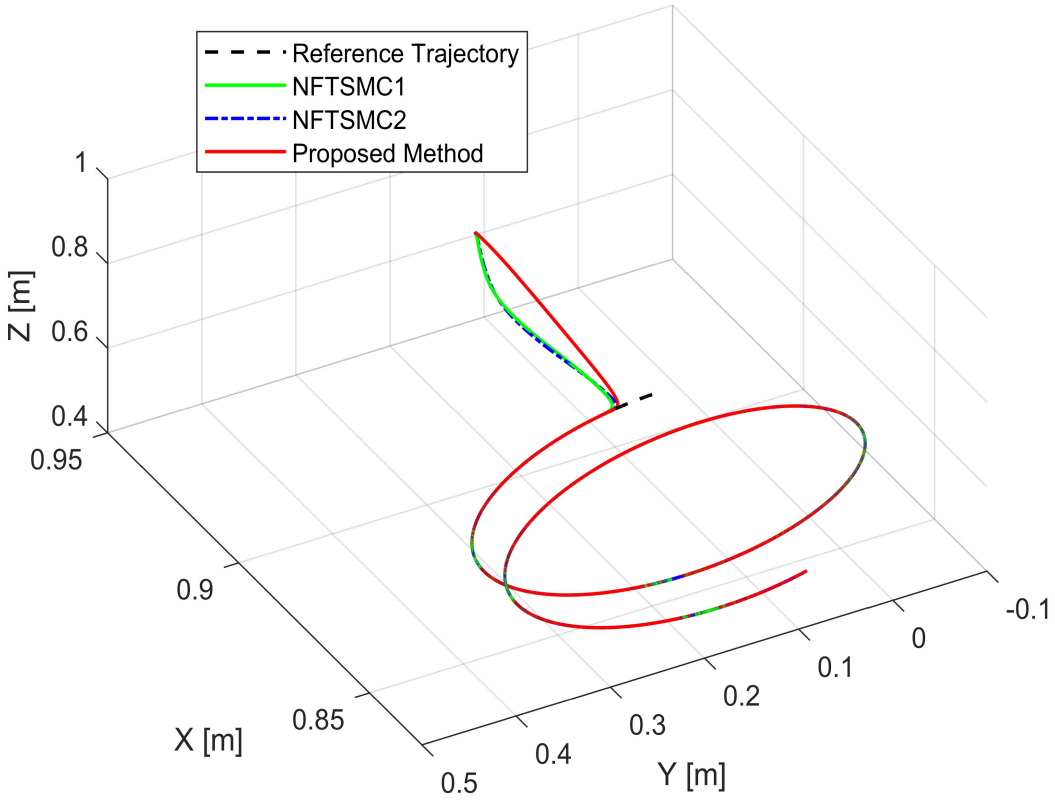

FIGURE 4. The real trajectory of the end effector position by tracking a specified path in 3-dimensional space (XYZ).

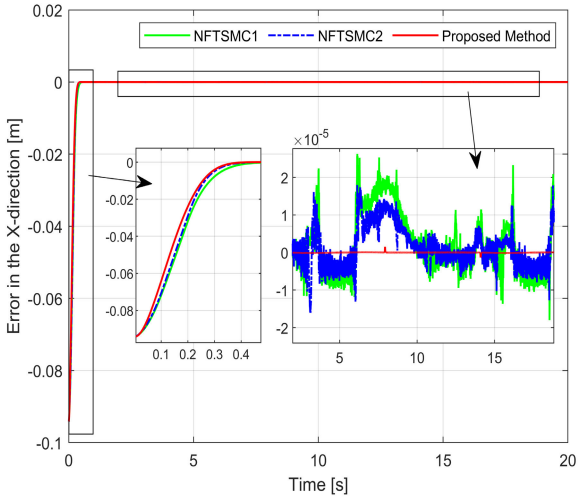

FIGURE 5. The error comparison between the trajectory of the end effector position versus reference trajectory along the X-axis.

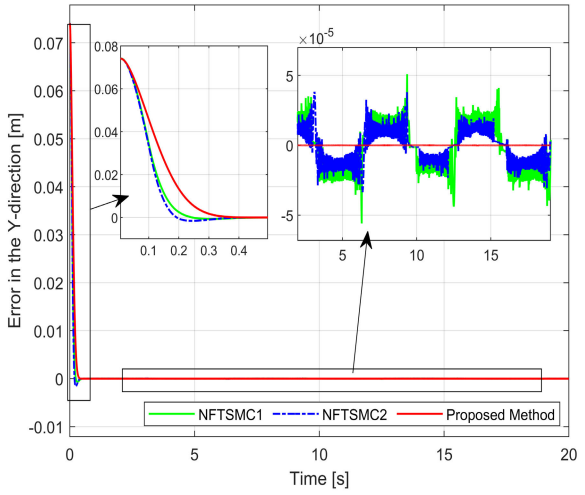

FIGURE 6. The error comparison between the trajectory of the end effector position versus reference trajectory along the Y-axis.

including tracking accuracy and convergence rate shown in Figs. 4 - 7. Judging from Figs. 4 - 7, it can be seen that all three control systems provide a high tracking accuracy with a rapid convergence rate in finite-time when all three methods are advanced control methods based on NFTSMC. NFTSMC2 in Eq. (39) was developed based on NFTSMC1 in Eq. (38). Therefore, NFTSMC2 has a little faster convergence rate and a little higher accuracy than those of NFTSMC1. Especially, the proposed controller was developed based on the NFTSMC2 combined with DO. Obviously, active control

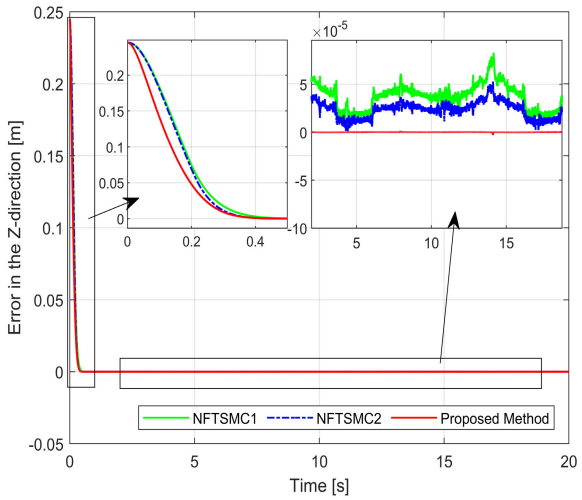

FIGURE 7. The error comparison between the trajectory of the end effector position versus reference trajectory along the Z-axis.

algorithms will provide higher tracking accuracy than that of passive controllers if the estimated information exactly offers to the control loop. As a result, the proposed control system has the highest tracking accuracy and the fastest convergence rate among the three control algorithms.

Third, a comparison of chattering behavior among the three different control methods was shown in Fig. 8. Oscillation phenomena appearing in both the NFTSMC1 and NFTSMC2 controller is very serious. They seem to have the same amplitude and frequency when applied same the sliding value ($\Delta_5^* = 13, v_5 = 0.1$ and $\Delta_6^* = 13, v_6 = 0.1$). In contrast, oscillation phenomena did not significantly appear in the control inputs of the proposed system. The proposed controller provided smooth control signals.

Final, by applying the dual layers adaptive algorithm in DO, the necessity of an upper bound of the lumped uncertainty was declined. It is observed from Fig. 9, the adaptation gain values are proportional to the variation of indeterminate components. It is not like regular adaptation approaches that only have an increase to attain the upper limit value of the lumped uncertainty.

B. EXPERIMENTAL PROCESS FOR TRAJECTORY TRACKING CONTROL OF AN UNCERTAIN MLS

Let us consider MLS displayed in Fig. 10. MLS's nonlinear model has been described in our published paper [67]:

$$\ddot{h} = g - \frac{\hat{\Gamma}}{h^2}u^2 + \Delta\left(h, t\right), \tag{40}$$

where h is the position of the metal sphere, g is the acceleration due to the gravity, and $\hat{\Gamma}$ is approximation value of the real value Γ. The real value $\Gamma = \sigma K^2/m$, m is a mass

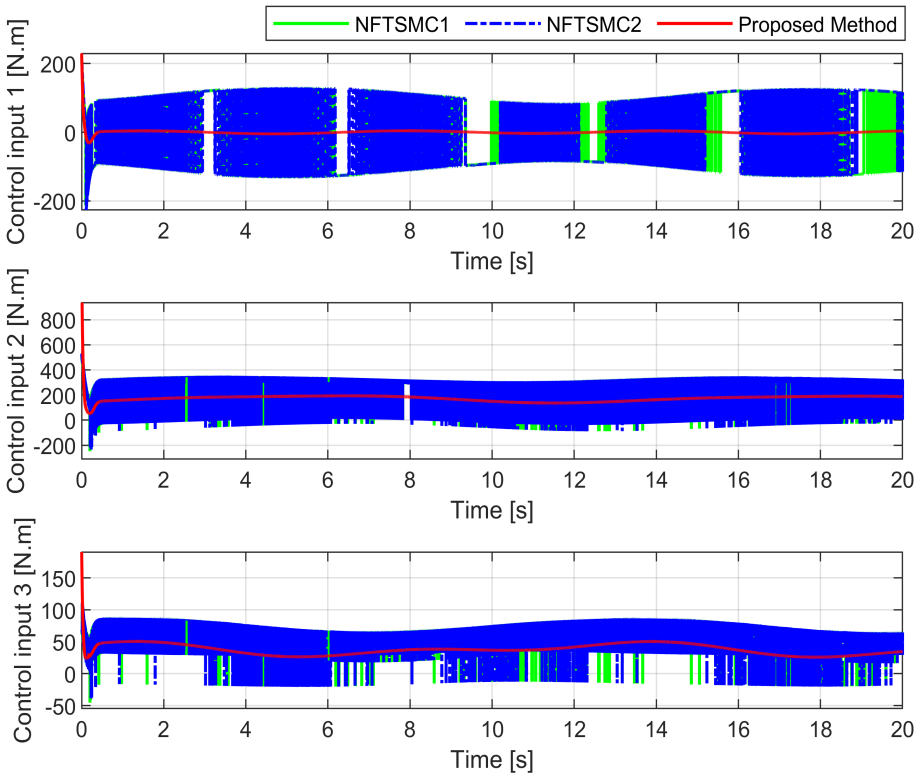

FIGURE 8. Comparison of chattering behavior among the three different control methods and their control signals.

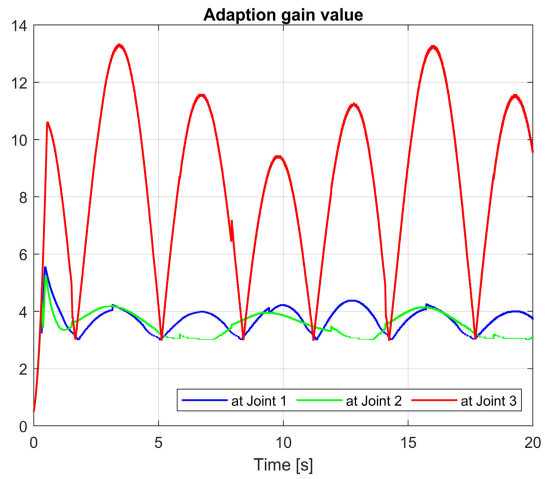

FIGURE 9. Adaptation gain value of $\Delta^*(t)$ at each Joint.

of the metal sphere, K is a relationship coefficient between the current flowing in winding i and the control voltage u, σ is a constant depending on the characteristics of the electromagnet, and $\Delta(h,t)$ is the lumped uncertainty.

We set $x = [x_1, x_2]^T = \left[h, \dot{h}\right]^T$, $a(x) = -\hat{\Gamma}\Big/h^2$, $b(x) = g$, and $\sqrt{u_d} = u$; accordingly, the modelling of MLS (40) is transferred in state space as:

$$\begin{cases} \dot{x}_1 = x_2 \\ \dot{x}_2 = a(x)\, u_d + b(x) + \Delta(x,t)\,. \end{cases} \tag{41}$$

Eq. (41) has a form of a second-order nonlinear system. Therefore, the proposed method can be directly applied to this MLS.

MLS in experiment is shown in Fig. 11. The system includes number 1) a mechanical component; number 2) analogue control interface; number 3) feedback SCSI adapter box; number 4) a PCI1711 I/O card.

The essential tools for implementation of the control algorithm were stated our published paper [67]. We set the system (38) with the nominal parameters according to [68] as $m = 0.02\ (kg)$, $\sigma = 2.48315625 \times 10^{-5}\ \left(Nm^2/A^2\right)$, $\hat{\Gamma} = 1.36884 \times 10^{-3}\ \left(N.m^2/kg.V^2\right)$, $g = 9.81\ \left(m/s^2\right)$, and $K = 1.05\ \left(A/V\right)$.

To verify the proposed controller performance by using experimental results, experiments for an MLS were performed under different operating conditions that include the following cases:

Case 1: An external disturbance is assumed as:

$$d(t) = 2\sin\left(\pi t/5\right)\ \left(m/s^2\right). \tag{42}$$

The metal sphere is controlled to track the following reference trajectory:

$$h_r = 15 + 2.5\sin\left(\pi t/10\right)\quad (mm)\,. \tag{43}$$

Case 2: An external disturbance of a different value is assumed as:

$$d(t) = 1\sin\left(\pi t/10\right) + 0.8\sin\left(\pi t/5\right) + 0.8\sin\left(2\pi t/5\right)\ \left(m/s^2\right). \tag{44}$$

The metal sphere is controlled to track the following reference trajectory:

$$h_r = 15 + 2.5\cos\left(7\pi t/50\right)\quad (mm)\,. \tag{45}$$

We have the initial value of $h_0 = 26\,(mm)$, $h_{r\min} = 12.5\,(mm)$, $u_{d\max} < 4.5\,(V)$, and $\Gamma = 1.34557 \times 10^{-3}$ (according to the experimental results in [68]). Accordingly, the following suitable assumption of the lumped uncertainty

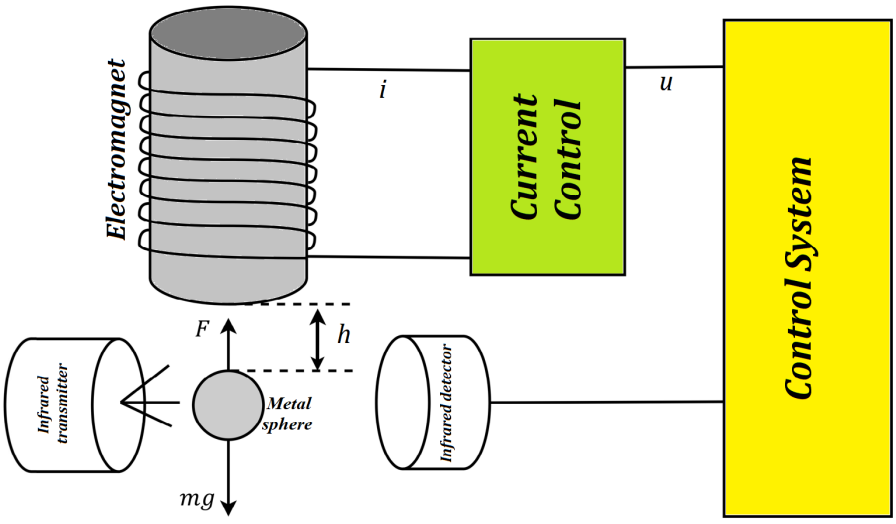

FIGURE 10. Description of a magnetic levitation system according to [59].

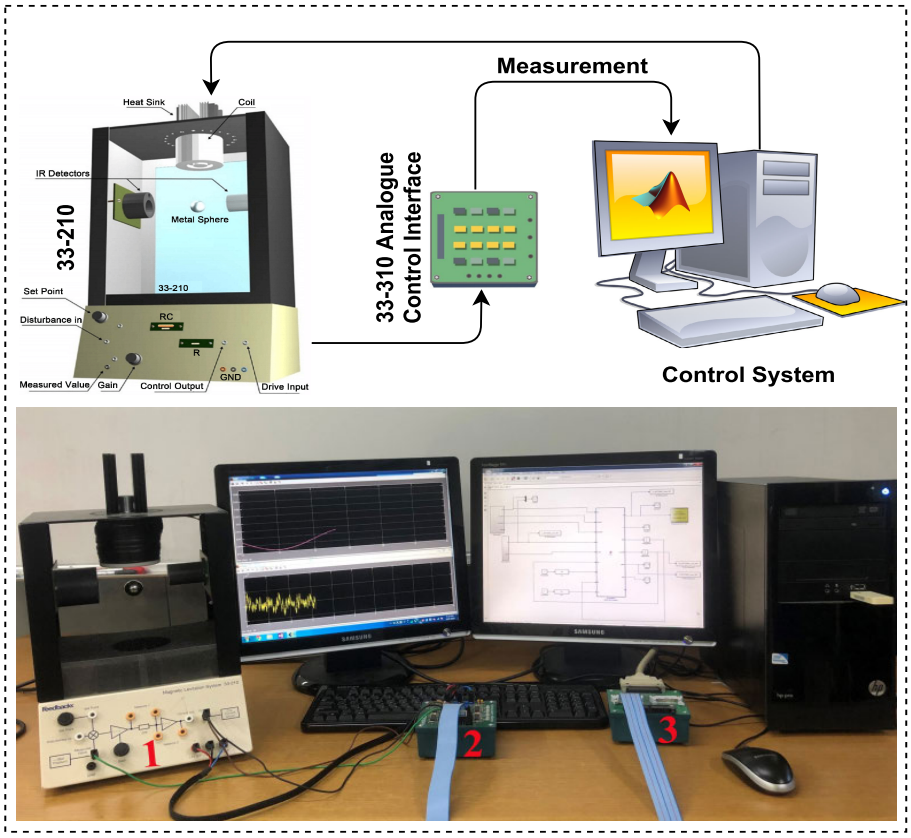

FIGURE 11. Setting up of the experimental system.

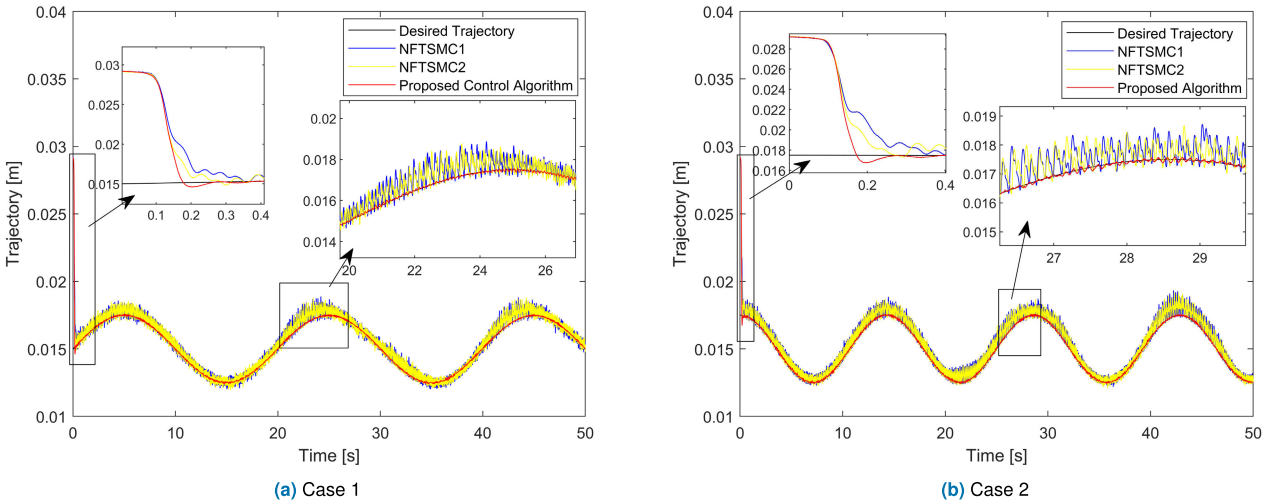

(a) Case 1 (b) Case 2

FIGURE 12. Position tracking performance of the metal sphere under three different control systems.

is described as:

$$\left|\dot{\Delta}\left(h,t\right)\right| \leqslant \frac{\left|\Gamma-\hat{\Gamma}\right|}{h_{\min}^{2}} u_{d\max}^{2} = 3. \tag{46}$$

The control inputs of NFTSMC1 based on [66] and NFTSMC2 based on [41] are synthesized for an uncertain MLS as:

$$\begin{cases} s = \dot{x}_e + \alpha_7 x_e + \beta_7 sig(x_e)^{\omega_7} \\ u = \sqrt{\dfrac{h^2}{\hat{\Gamma}}\begin{pmatrix} g - \ddot{h}_r + \left(\alpha_7 + \beta_7\omega_7 |x_e|^{\omega_7 - 1}\right)\dot{x}_e \\ +\Lambda_7 s + \left(\Delta_7^* + v_7\right)\mathrm{sgn}\left(s\right) \end{pmatrix}} \end{cases} \tag{47}$$

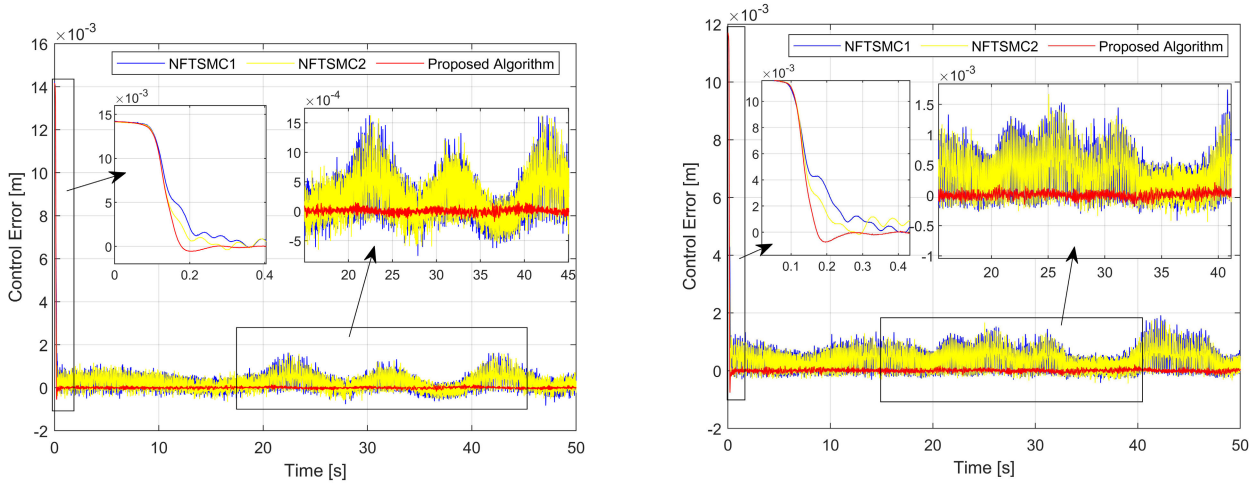

(a) Case 1 (b) Case 2

FIGURE 13. The error comparison between the trajectory of the metal sphere and reference trajectory.

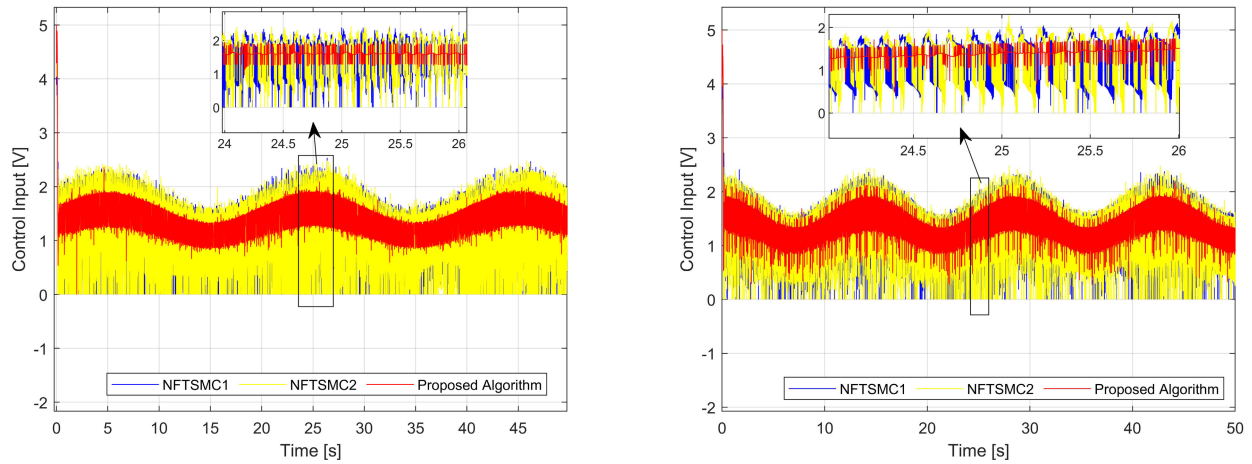

(a) Case 1 (b) Case 2

FIGURE 14. The response of the output voltage under three different control systems.

and

$$\begin{cases} s = \dot{x}_e + \dfrac{2\alpha_8}{1+e^{-\eta_8(|x_e|-\varepsilon_8)}}x_e + \dfrac{2\beta_8}{1+e^{\mu_8(|x_e|-\varepsilon_8)}}sig(x_e)^{\omega_8} \\ u = \sqrt{\dfrac{h^2}{\hat{\Gamma}}\left(\begin{array}{l} g - \ddot{h}_r + \dfrac{2\alpha_8}{1+e^{-\eta_8(|x_e|-\varepsilon_8)}}\dot{x}_e \\ + \dfrac{2\alpha_8\eta_8\dot{x}_e\,\mathrm{sgn}\,(x_e)\,e^{-\eta_8(|x_e|-\varepsilon_8)}}{\left(1+e^{-\eta_8(|x_e|-\varepsilon_8)}\right)^2}x_e \\ + \dfrac{2\beta_8\omega_8}{1+e^{\mu_8(|x_e|-\varepsilon_8)}}|x_e|^{\omega_8-1}\dot{x}_e \\ - \dfrac{2\beta_8\mu_8\dot{x}_e e^{\mu_8(|x_e|-\varepsilon_8)}}{\left(1+e^{\mu_8(|x_e|-\varepsilon_6)}\right)^2}|x_e|^{\omega_8} \\ +\Lambda_8 s + \left(\Delta_8^* + v_8\right)\mathrm{sgn}\,(s) \end{array}\right)} \end{cases}, \tag{48}$$

TABLE 2. Control parameter selection of control algorithms.

Algorithm	Control Parameters
NFTSMC1	$\alpha_7 = 5,\ \beta_7 = 5,\ \omega_7 = 0.8,\ \Lambda_7 = 50,\ \Delta_7^* = 5, v_7 = 0.1$
NFTSMC2	$\alpha_8 = 5,\ \beta_8 = 5,\ \eta_8 = 0.2, \mu_8 = 1.4, \omega_8 = 0.8, \Lambda_8 = 50,\ \Delta_8^* = 5, v_8 = 0.1$
Proposed Algorithm	Eq. (19): $\alpha_1 = 5,\ \beta_1 = 5,\ \eta_1 = 0.2,\ \mu_1 = 1.4, \omega_1 = 0.8$ Eq. (26): $\alpha_2 = 50,\ \beta_2 = 10,\ \varphi_2 = 1.6,\ \lambda_2 = 0.8$ Eqs. (11) and (12): $\alpha_3 = 2,\ \beta_3 = 2,\ \eta_3 = 0.8,\ \mu_3 = 1.2, \omega_3 = 0.8, \alpha_4 = 3,\ \beta_4 = 3,\ \eta_4 = 0.8,\ \mu_4 = 1.2, \omega_4 = 0.8$ Eqs. (17) and (18): $\Delta_0 = 2, \Delta_d = 5, \psi_0 = 0.5, \rho = 4, k_0 = 0.8, k_1 = 0.6, \kappa = 0.8, \theta = 0.7$

where $x_e = h - h_r$, $\alpha_7, \alpha_8, \beta_7, \beta_8, \eta_8, \mu_8$ are the design positive constants, $0 < \omega_7, \omega_8 < 1$, $\varepsilon_8 = \left(\beta_8/\alpha_8\right)^{1/(1-\omega_8)}$. $\left(\Delta_7^* + v_7\right)$ and $\left(\Delta_8^* + v_8\right)$ are positive constants.

Control parameter selection of the three control algorithms in the experimental example is reported in Table 2.

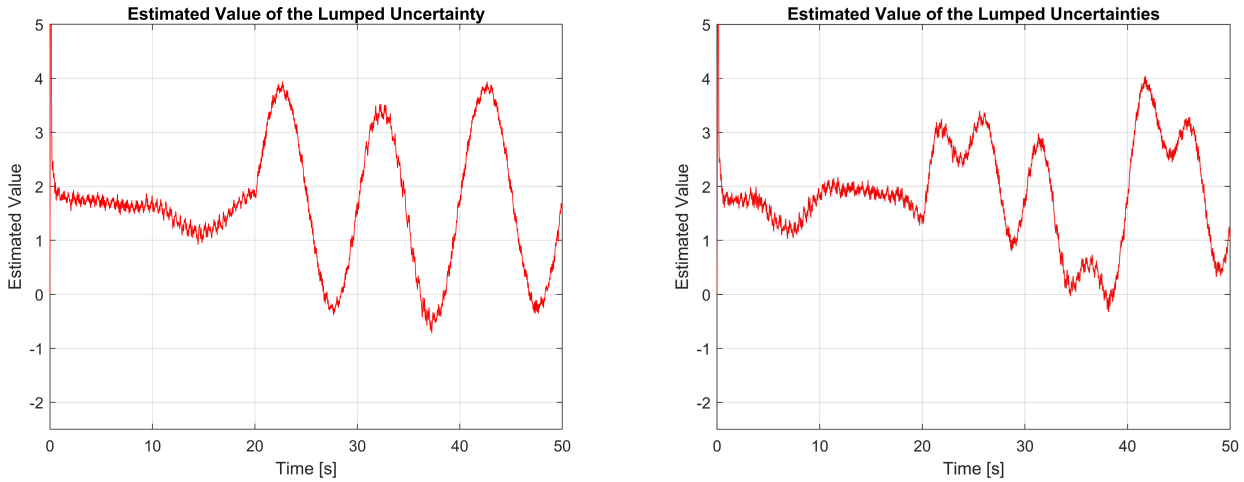

(a) Case 1 (b) Case 2

FIGURE 15. Approximation value of the lumped uncertainty.

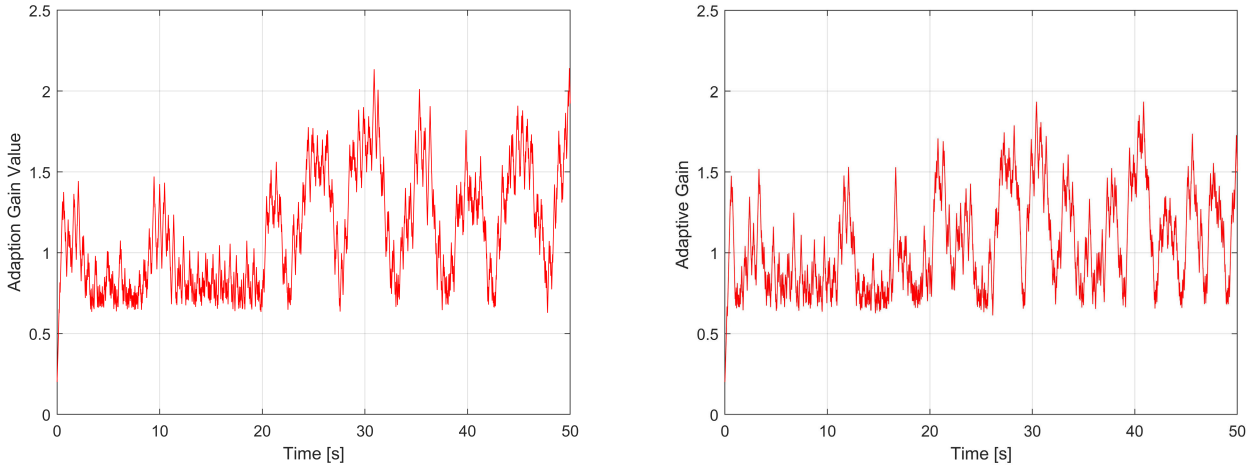

(a) Case 1 (b) Case 2

FIGURE 16. Adaptation gain value of $\Delta^*(t)$.

Investigation of the control performance under the three control algorithms was performed in two stages:

Stage 1: When $0 < t < 20$ (s), MLS only is checked with the dynamical uncertain term without the influences of exterior disturbances $(d(t) = 0)$.

Stage 2: When $t \geqslant 20$ (s), an assumed disturbance is added to MLS. Specifically, in both cases, the assumed value of the external disturbance is respectively given in Eqs. (42) and (44).

The tracking position of the metal sphere in both cases is displayed in Fig. 12. In comparison with the desired trajectory, the trajectory error of the metal sphere under each control algorithm is exhibited in Fig. 12. Fig. 12 displays that all three control methodologies offered high tracking precision with fast convergence in finite-time. Judging the tracking error produced by the three control approaches in Fig. 13, it is observed that NFTSMC1 and NFTSMC2 offered the similar tracking errors. The accuracy from the position tracking of both methods has been attained which is on the order of $10^{-3} \sim 10^{-4}$ (m). And their convergence time has been also attained $T \approx 0.3$ (s). Nonetheless, NFTSMC2 has a little faster convergence time than that of NFTSMC1. It is noteworthy that the proposed control methodology has the best performance in two terms including the tracking errors $(10^{-4} \sim 10^{-5}$ $(m))$ and convergence time $(T \approx 0.2$ $(s))$ among the three control approaches.

Fig. 14 shows the control input signals of three different control methods. The chattering is also clearly displayed in Fig. 14. In comparison of chattering phenomena among the three control approaches, Chattering occurred in the control signals of both NFTSMC1 and NFTSMC2 has the same amplitude and frequency. Because NFTSMC1 and

NFTSMC2 have applied the same sliding value ($\Delta_7^* = 5, v_7 = 0.1$ and $\Delta_8^* = 5, v_8 = 0.1$) in the reaching control law to dismiss the undesired influences of the lumped uncertainty. Chattering still occurred in the control signal of the designed control algorithm due to the characteristic of MLS to keep the metal sphere suspended in the air. However, the amplitude and frequency of the chattering was significantly reduced.

Fig. 15 displays the approximated value of the lumped uncertainty. As shown Fig. 15, DO has a fast convergence in finite-time. Consequently, the convergence time of DO is ensured to prevent delays in providing the necessary knowledge of the lumped uncertainty to the control system.

The approximation value of $\Delta^*(t)$ is illustrated in Fig. 16. Fig. 16 indicates that the adaptation gain value is excellently adapted according to alterations of the lumped uncertainty. From simulated and experimental evaluation results, the control proposal proved to be the best of the three control methods in three aspects including accuracy in trajectory tracking, fast finite-time convergence, and chattering alleviation.

Remark 3: The selection and achievement of the excellent control parameters for all three control schemes shall be subject to the following conditions: first, shall be in accordance with the conditions given in the paper; second, to ensure fairness of comparison between all three control methods; finally, the selection of the control parameters is carried out by a series of repeated tests to obtain the best control performance in terms of high tracking accuracy, rapid finite-time convergence, and chattering phenomena decrease.

V. CONCLUSION

A novel tracking control algorithm using a finite-time disturbance observer was designed in this paper which obtained fast convergence within a predetermined amount of time and strong stability for a class of second-order nonlinear systems. Firstly, a nonlinear sliding mode manifold with fast finite-time convergence was introduced. Then, according to the designed manifold for the guarantee of finite-time convergence and robustness stabilization, a nonlinear control algorithm based on theory of finite-time control was developed. Specifically, the information of the lumped uncertainty was achieved by a new finite-time DO. The bounded value of the convergence time of the sliding manifold, DO, as well as the control system, were found from the theory of finite-time stability and Lyapunov stability approach. Thanks to the synthetic advantages of the above techniques, the designed system marked with powerful features including a practical design, fast convergence rate, high precision, a convergence of the control errors in finite-time, along with impressive small chattering in the control actions. The control proposal also eliminates the necessity of the upper boundary of the uncertainties affecting the system.

Our algorithm has proved to be the best of the three control algorithms from simulated and experimental performance in three aspects including accuracy in trajectory tracking, fast finite-time convergence, and chattering alleviation. The proposed method has proven highly effective and applicable to a class of second-order nonlinear systems.

In the simulation for a robot system, although the achieved dynamic model of this robot completely like the actual dynamic model, the proposed method has not been applied to actual robot systems. Therefore, our next goal is to verify the effectiveness of the proposed method using a real robotic system.

REFERENCES

[1] M. Van and D. Ceglarek, "Robust fault tolerant control of robot manipulators with global fixed-time convergence," *J. Franklin Inst.*, vol. 358, no. 1, pp. 699–722, Jan. 2021.

[2] K. Rudin, G. J. J. Ducard, and R. Y. Siegwart, "Active fault-tolerant control with imperfect fault detection information: Applications to UAVs," *IEEE Trans. Aerosp. Electron. Syst.*, vol. 56, no. 4, pp. 2792–2805, Aug. 2019.

[3] X. Zhu, Y. Xia, and M. Fu, "Fault estimation and active fault-tolerant control for discrete-time systems in finite-frequency domain," *ISA Trans.*, vol. 104, pp. 184–191, Sep. 2020.

[4] A. Qiu, A. W. Al-Dabbagh, H. Yu, and T. Chen, "A design framework for event-triggered active fault-tolerant control systems," *Int. J. Control*, pp. 1–12, 2020, doi: 10.1080/00207179.2020.1713401.

[5] A. Guezmil, H. Berriri, R. Pusca, A. Sakly, R. Romary, and M. F. Mimouni, "Experimental investigation of passive fault tolerant control for induction machine using sliding mode approach," *Asian J. Control*, vol. 21, no. 1, pp. 520–532, Jan. 2019.

[6] H. R. Patel and V. A. Shah, "Performance comparison of passive fault tolerant control strategy with PI and fuzzy control of single-tank level process with sensor and system fault," *Amer. J. Eng. Appl. Sci.*, vol. 12, no. 2, pp. 236–246, Feb. 2019.

[7] H. Hammouri, G. Bornard, and K. Busawon, "High gain observer for structured multi-output nonlinear systems," *IEEE Trans. Autom. Control*, vol. 55, no. 4, pp. 987–992, Apr. 2010.

[8] H. K. Khalil, "Cascade high-gain observers in output feedback control," *Automatica*, vol. 80, pp. 110–118, Jun. 2017.

[9] X.-G. Yan and C. Edwards, "Nonlinear robust fault reconstruction and estimation using a sliding mode observer," *Automatica*, vol. 43, no. 9, pp. 1605–1614, Sep. 2007.

[10] Y. Yin, J. Liu, J. A. Sanchez, L. Wu, S. Vazquez, J. I. Leon, and L. G. Franquelo, "Observer-based adaptive sliding mode control of NPC converters: An RBF neural network approach," *IEEE Trans. Power Electron.*, vol. 34, no. 4, pp. 3831–3841, Apr. 2019.

[11] C. Hua, C. Yu, and X. Guan, "Neural network observer-based networked control for a class of nonlinear systems," *Neurocomputing*, vol. 133, pp. 103–110, Jun. 2014.

[12] A. T. Vo and H.-J. Kang, "A novel fault-tolerant control method for robot manipulators based on non-singular fast terminal sliding mode control and disturbance observer," *IEEE Access*, vol. 8, pp. 109388–109400, 2020.

[13] H. Pan, W. Sun, H. Gao, and X. Jing, "Disturbance observer-based adaptive tracking control with actuator saturation and its application," *IEEE Trans. Autom. Sci. Eng.*, vol. 13, no. 2, pp. 868–875, Apr. 2016.

[14] G. Besançon, *Nonlinear Observers and Applications*, vol. 363. Berlin, Germany: Springer, 2007, doi: 10.1007/978-3-540-73503-8.

[15] J.-H. Park, S.-H. Kim, and T.-S. Park, "Approximation-free output-feedback control of uncertain nonlinear systems using higher-order sliding mode observer," *J. Dyn. Syst., Meas., Control*, vol. 140, no. 12, Dec. 2018.

[16] J.-H. Park, S.-H. Kim, and T.-S. Park, "Output-feedback adaptive neural controller for uncertain pure-feedback nonlinear systems using a high-order sliding mode observer," *IEEE Trans. Neural Netw. Learn. Syst.*, vol. 30, no. 5, pp. 1596–1601, May 2019.

[17] P. V. Suryawanshi, P. D. Shendge, and S. B. Phadke, "A boundary layer sliding mode control design for chatter reduction using uncertainty and disturbance estimator," *Int. J. Dyn. Control*, vol. 4, no. 4, pp. 456–465, Dec. 2016.

[18] A. Sahamijoo, F. Piltan, M. H. Mazloom, M. R. Avazpour, H. Ghiasi, and N. B. Sulaiman, "Methodologies of chattering attenuation in sliding mode controller," *Int. J. Hybrid Inf. Technol.*, vol. 9, no. 2, pp. 11–36, Feb. 2016.

[19] R. Seeber, M. Horn, and L. Fridman, "A novel method to estimate the reaching time of the super-twisting algorithm," *IEEE Trans. Autom. Control*, vol. 63, no. 12, pp. 4301–4308, Dec. 2018.

[20] A. Swikir and V. Utkin, "Chattering analysis of conventional and super twisting sliding mode control algorithm," in *Proc. 14th Int. Workshop Variable Struct. Syst. (VSS)*, Jun. 2016, pp. 98–102.
[21] A. Goel and A. Swarup, "Chattering free trajectory tracking control of a robotic manipulator using high order sliding mode," in *Advances in Computer and Computational Sciences* (Advances in Intelligent Systems and Computing), vol. 553, S. Bhatia, K. Mishra, S. Tiwari, and V. Singh, Eds. Singapore: Springer, 2017, doi: 10.1007/978-981-10-3770-2_71.
[22] Q. V. Doan, T. D. Le, and A. T. Vo, "Synchronization full-order terminal sliding mode control for an uncertain 3-DOF planar parallel robotic manipulator," *Appl. Sci.*, vol. 9, no. 9, p. 1756, Apr. 2019.
[23] A. T. Vo and H.-J. Kang, "Adaptive neural integral full-order terminal sliding mode control for an uncertain nonlinear system," *IEEE Access*, vol. 7, pp. 42238–42246, 2019.
[24] A. T. Vo and H.-J. Kang, "A chattering-free, adaptive, robust tracking control scheme for nonlinear systems with uncertain dynamics," *IEEE Access*, vol. 7, pp. 10457–10466, 2019.
[25] S. K. Kommuri, S. B. Lee, and K. C. Veluvolu, "Robust sensors-fault-tolerance with sliding mode estimation and control for PMSM drives," *IEEE/ASME Trans. Mechatronics*, vol. 23, no. 1, pp. 17–28, Feb. 2018.
[26] W. Bai, Q. Zhou, T. Li, and H. Li, "Adaptive reinforcement learning neural network control for uncertain nonlinear system with input saturation," *IEEE Trans. Cybern.*, vol. 50, no. 8, pp. 3433–3443, Aug. 2020.
[27] X. Zhao, X. Wang, L. Ma, and G. Zong, "Fuzzy approximation based asymptotic tracking control for a class of uncertain switched nonlinear systems," *IEEE Trans. Fuzzy Syst.*, vol. 28, no. 4, pp. 632–644, Apr. 2020.
[28] M. Chen, S.-Y. Shao, and B. Jiang, "Adaptive neural control of uncertain nonlinear systems using disturbance observer," *IEEE Trans. Cybern.*, vol. 47, no. 10, pp. 3110–3123, Oct. 2017.
[29] A. T. Vo and H.-J. Kang, "Neural integral non-singular fast terminal synchronous sliding mode control for uncertain 3-DOF parallel robotic manipulators," *IEEE Access*, vol. 8, pp. 65383–65394, 2020.
[30] M. Van and S. S. Ge, "Adaptive fuzzy integral sliding mode control for robust fault tolerant control of robot manipulators with disturbance observer," *IEEE Trans. Fuzzy Syst.*, early access, Feb. 13, 2020, doi: 10.1109/TFUZZ.2020.2973955.
[31] C. Edwards and S. Spurgeon, *Sliding Mode Control: Theory and Applications*. Boca Raton, FL, USA: CRC Press, 1998.
[32] J. Liu, Y. Gao, X. Su, M. Wack, and L. Wu, "Disturbance-observer-based control for air management of PEM fuel cell systems via sliding mode technique," *IEEE Trans. Control Syst. Technol.*, vol. 27, no. 3, pp. 1129–1138, May 2019.
[33] S. Liu, Y. Liu, and N. Wang, "Nonlinear disturbance observer-based backstepping finite-time sliding mode tracking control of underwater vehicles with system uncertainties and external disturbances," *Nonlinear Dyn.*, vol. 88, no. 1, pp. 465–476, Apr. 2017.
[34] W. Liu and P. Li, "Disturbance observer-based fault-tolerant adaptive control for nonlinearly parameterized systems," *IEEE Trans. Ind. Electron.*, vol. 66, no. 11, pp. 8681–8691, Nov. 2019.
[35] A. Vahidi-Moghaddam, A. Rajaei, and M. Ayati, "Disturbance-observer-based fuzzy terminal sliding mode control for MIMO uncertain nonlinear systems," *Appl. Math. Model.*, vol. 70, pp. 109–127, Jun. 2019.
[36] J. Liu and X. Wang, *Advanced Sliding Mode Control for Mechanical Systems*. Berlin, Germany: Springer-Verlag, 2012, doi: 10.1007/978-3-642-20907-9.
[37] S. Amirkhani, S. Mobayen, N. Iliaee, O. Boubaker, and S. H. Hosseinnia, "Fast terminal sliding mode tracking control of nonlinear uncertain mass–spring system with experimental verifications," *Int. J. Adv. Robot. Syst.*, vol. 16, no. 1, 2019, Art. no. 1729881419828176.
[38] W. Liu, Z. Feng, and A. Bi, "A novel nonsingular terminal sliding mode control combined with global sliding surface for uncertain nonlinear second-order systems," *Trans. Inst. Meas. Control*, vol. 42, no. 2, 2019, Art. no. 0142331219889172.
[39] J. Liu and F. Sun, "A novel dynamic terminal sliding mode control of uncertain nonlinear systems," *J. Control Theory Appl.*, vol. 5, no. 2, pp. 189–193, May 2007.
[40] S. Yu, G. Guo, Z. Ma, and J. Du, "Global fast terminal sliding mode control for robotic manipulators," *Int. J. Model. Identifcation Control*, vol. 1, no. 1, pp. 72–79, 2006.
[41] H. Pan, G. Zhang, H. Ouyang, and L. Mei, "A novel global fast terminal sliding mode control scheme for second-order systems," *IEEE Access*, vol. 8, pp. 22758–22769, 2020.
[42] H. Pan and W. Sun, "Nonlinear output feedback finite-time control for vehicle active suspension systems," *IEEE Trans. Ind. Informat.*, vol. 15, no. 4, pp. 2073–2082, Apr. 2019.
[43] L. Qiao and W. Zhang, "Double-loop integral terminal sliding mode tracking control for UUVs with adaptive dynamic compensation of uncertainties and disturbances," *IEEE J. Ocean. Eng.*, vol. 44, no. 1, pp. 29–53, Jan. 2019.
[44] L. Qiao and W. Zhang, "Trajectory tracking control of AUVs via adaptive fast nonsingular integral terminal sliding mode control," *IEEE Trans. Ind. Informat.*, vol. 16, no. 2, pp. 1248–1258, Feb. 2020.
[45] X. Yao, J. H. Park, H. Dong, L. Guo, and X. Lin, "Robust adaptive nonsingular terminal sliding mode control for automatic train operation," *IEEE Trans. Syst. Man, Cybern. Syst.*, vol. 49, no. 12, pp. 2406–2415, Dec. 2018.
[46] C. Jing, H. Xu, X. Niu, and X. Song, "Adaptive nonsingular terminal sliding mode control for attitude tracking of spacecraft with actuator faults," *IEEE Access*, vol. 7, pp. 31485–31493, 2019.
[47] S. Ding, L. Liu, and J. H. Park, "A novel adaptive nonsingular terminal sliding mode controller design and its application to active front steering system," *Int. J. Robust Nonlinear Control*, vol. 29, no. 12, pp. 4250–4269, Jun. 2019.
[48] J. Zhang, Y. Lin, and G. Feng, "Analysis and synthesis of memory-based fuzzy sliding mode controllers," *IEEE Trans. Cybern.*, vol. 45, no. 12, pp. 2880–2889, Dec. 2015.
[49] S. Mondal and C. Mahanta, "Adaptive second order terminal sliding mode controller for robotic manipulators," *J. Franklin Inst.*, vol. 351, no. 4, pp. 2356–2377, Apr. 2014.
[50] S. Mobayen and F. Tchier, "A novel robust adaptive second-order sliding mode tracking control technique for uncertain dynamical systems with matched and unmatched disturbances," *Int. J. Control, Autom. Syst.*, vol. 15, no. 3, pp. 1097–1106, Jun. 2017.
[51] A. T. Vo, H.-J. Kang, and V.-C. Nguyen, "An output feedback tracking control based on neural sliding mode and high order sliding mode observer," in *Proc. 10th Int. Conf. Hum. Syst. Interact. (HSI)*, Jul. 2017, pp. 161–165.
[52] J. Liu and X. Wang, *Advanced Sliding Mode Control for Mechanical Systems: Design, Analysis and MATLAB Simulation*. Berlin, Germany: Springer-Verlag, 2012, doi: 10.1007/978-3-642-20907-9.
[53] A. T. Vo and H.-J. Kang, "An adaptive neural non-singular fast-terminal sliding-mode control for industrial robotic manipulators," *Appl. Sci.*, vol. 8, no. 12, p. 2562, Dec. 2018.
[54] P. S. Londhe and B. M. Patre, "Adaptive fuzzy sliding mode control for robust trajectory tracking control of an autonomous underwater vehicle," *Intell. Service Robot.*, vol. 12, no. 1, pp. 87–102, Jan. 2019.
[55] M. Vijay and D. Jena, "PSO based neuro fuzzy sliding mode control for a robot manipulator," *J. Electr. Syst. Inf. Technol.*, vol. 4, no. 1, pp. 243–256, May 2017.
[56] A. T. Vo, H.-J. Kang, and T. D. Le, "An adaptive fuzzy terminal sliding mode control methodology for uncertain nonlinear second-order systems," in *Proc. Int. Conf. Intell. Comput.*, 2018, pp. 123–135.
[57] S. B. Niku, *Introduction to Robotics: Analysis, Control, Applications*. Hoboken, NJ, USA: Wiley, 2020.
[58] B. Armstrong, O. Khatib, and J. Burdick, "The explicit dynamic model and inertial parameters of the PUMA 560 arm," in *Proc. IEEE Int. Conf. Robot. Automat.*, vol. 3, Apr. 1986, pp. 510–518.
[59] M. B. Naumović and B. R. Veselić, "Magnetic levitation system in control engineering education," *FACTA Univ. Ser. Autom. Control Robot.*, vol. 7, no. 1, pp. 151–160, 2008.
[60] Z. Zhao, X. He, and C. K. Ahn, "Boundary disturbance observer-based control of a vibrating single-link flexible manipulator," *IEEE Trans. Syst., Man, Cybern. Syst.*, early access, May 7, 2019, doi: 10.1109/TSMC.2019.2912900.
[61] B. Jiang, M. Staroswiecki, and V. Cocquempot, "Fault accommodation for nonlinear dynamic systems," *IEEE Trans. Autom. Control*, vol. 51, no. 9, pp. 1578–1583, Sep. 2006.
[62] Z. Zuo, "Non-singular fixed-time terminal sliding mode control of non-linear systems," *IET Control theory Appl.*, vol. 9, no. 4, pp. 545–552, 2014.
[63] C. Edwards and Y. Shtessel, "Adaptive dual-layer super-twisting control and observation," *Int. J. Control*, vol. 89, no. 9, pp. 1759–1766, Sep. 2016.
[64] H. Pan, G. Zhang, H. Ouyang, and L. Mei, "Novel fixed-time non-singular fast terminal sliding mode control for second-order uncertain systems based on adaptive disturbance observer," *IEEE Access*, vol. 8, pp. 126615–126627, 2020.
[65] V. Utkin and J. Y. Gulder, *Sliding Mode Control in Electro-Mechanical Systems*. New York, NY, USA: Taylor & Francis, 1999.

[66] X. Yu and M. Zhihong, "Fast terminal sliding-mode control design for nonlinear dynamical systems," *IEEE Trans. Circuits Syst. I, Fundam. Theory Appl.*, vol. 49, no. 2, pp. 261–264, Feb. 2002.
[67] T. N. Truong, A. T. Vo, and H.-J. Kang, "Implementation of an adaptive neural terminal sliding mode for tracking control of magnetic levitation systems," *IEEE Access*, vol. 8, pp. 206931–206941, 2020.
[68] R. Morales, V. Feliu, and H. Sira-Ramírez, "Nonlinear control for magnetic levitation systems based on fast online algebraic identification of the input gain," *IEEE Trans. Control Syst. Technol.*, vol. 19, no. 4, pp. 757–771, Jul. 2011.

ANH TUAN VO received the B.S. degree in electrical engineering from the Da Nang University of Technology, Da Nang, Vietnam, in 2008, the M.S. degree in automation from The University of Danang - University of Science and Technology, Da Nang, in 2013, and the Ph.D. degree in electrical engineering from the Graduate School, University of Ulsan, Ulsan, South Korea, in 2021. He has published more than 20 articles in journals and international conferences. His research interests include intelligent control, sliding mode control and its application, and fault-tolerant control.

THANH NGUYEN TRUONG received the B.S. degree in electrical engineering from the University of Science and Technology, Da Nang, Vietnam, in 2018. He is currently pursuing the Ph.D. degree with the University of Ulsan, Ulsan, South Korea. His research interests include robotic manipulators, sliding mode control and its application, and advanced control theory for mechatronics.

HEE-JUN KANG received the B.S. degree in mechanical engineering from Seoul National University, South Korea, in 1985, and the M.S. and Ph.D. degrees in mechanical engineering from The University of Texas at Austin, USA, in 1988 and 1991, respectively. Since 1992, he has been a Professor of electrical engineering with the University of Ulsan. His current research interests include sensor-based robotic application, robot calibration, haptics, robot fault diagnosis, and mechanism analysis.